10-16-2020

Role of ceramide-1 phosphate in regulation of sphingolipid and eicosanoid metabolism in lung epithelial cells

Brittany A. Dudley
University of South Florida

Role of ceramide-1 phosphate in regulation of sphingolipid and eicosanoid metabolism in lung epithelial cells

by

Brittany A. Dudley

A thesis submitted in partial fulfillment
of the requirements for the degree of
Master of Science
with a concentration in Cell and Molecular Biology
Department of Cell Biology, Microbiology and Molecular Biology
College of Arts and Sciences
University of South Florida

Major Professor: Charles Chalfant, Ph.D.
Margaret Park, Ph.D.
Sandy Westerheide, Ph.D.

Date of Approval:
October 14th, 2020

Keywords: Lipidomics, Cell Metabolism, Acid Sphingomyelinase, Inflammation

DEDICATION

This thesis is dedicated to the people who have supported me the most. My amazing mother, who inspires me every day to do my best. My father, whose initial doubt in my scientific abilities fueled me each and every day to prove him wrong. My brothers Brent, Mikey and Jeremy, each brought a smile to my face when I needed it the most. Above all, to the next generation of female scientists, never give up.

ACKNOWLEDGEMENTS

I would like to thank my amazing mentor and PI Dr. Charles Chalfant, for his consistent guidance and support. I first joined his laboratory towards the end of my undergraduate career. I became fascinated in his previous work, delving into lipidomics. He taught me essential life skills, such as scientific techniques, grant writing, and data analysis, which I honed during my graduate career. Thank you for feeding the flame, my passion for science, for entrusting me with projects which progressed to my thesis.

My sincerest thanks to committee members Dr. Margaret Park and Dr. Sandy Westerheide for being an essential part of my graduate experience, for being outstanding professors in my undergraduate and graduate classes, as well as providing essential feedback during my thesis process. I would like to thank Dr. Minjung Kim, for always willing to help out and make time to review data and questions regarding my thesis. I look up to these women, I aspire to be as successful, humble and gracious as they are.

Each semester, I had the opportunity of working as a teaching assistant to waive tuition fees. I would like to thank Mrs. Colbi Gemmell and Dr. William Brazelle for being fabulous lab coordinators, always willing to make time for students and help facilitate teaching labs. I would like to thank my students in both Anatomy and Physiology I and II labs, for giving me hope for the next generation of healthcare professionals.

The collaborative environment of Chalfant Lab enabled me to work hard and try my best to obtain as much data as possible each and every day. I would like to thank my coworkers, Anika Ali, Kenneth Maus, Melissa Berwick, Lauren Hawkins, and Christopher

Cardona, for taking the time to teach me new assays, provide feedback on my data, and willingness to work long hours to obtain statistically significant data. Our coffee runs together brought stress relief when I needed it the most, as well as new ideas for experimentation. Special thanks to coworker Dr. Daniel Stephenson for taking the time to teach me essential lipid extraction techniques, how to run samples on high-performance lipid chromatography and tandem mass spectrometry, identifying amount of analyte per sample, and quantifying this data for my thesis. I am so thankful for these colleagues and cannot imagine my graduate career without them.

TABLE OF CONTENTS

LIST OF TABLES

LIST OF FIGURES

ABSTRACT

Ceramide 1-Phosphate (C1P) is a sphingolipid metabolite which plays a large role in inflammation, cell survival and proliferation[1]. C1P is known to have both pro- and anti-apoptotic roles in lung cancer cells, governed by ceramide kinase (CERK), upstream of precursor ceramide (Cer)[2]. Previous work reveals C1P serves as the liaison between sphingolipid and eicosanoid synthesis, by decreasing the dissociation rate of group IVA cytosolic PLA_2 ($cPLA_{2\alpha}$) from the Golgi membrane, C1P directly activates this phospholipase for downstream eicosanoid synthesis and subsequent inflammatory response[3]. CERK has been discovered to modulate eicosanoid synthesis, elucidating upstream enzymes may have similar regulation[4]. It is unknown the specifics behind C1P anabolism and catabolism, such as which isoform of ceramide synthase (CerS) yields the primary chain length of Cer for C1P synthesis, and exploration of the elusive phosphatases responsible for converting C1P back to Cer. The total amount of C1P which derives from the de novo pathway is unknown.

In this study, **we hypothesize that ceramide synthase-1 and lipid phosphate phosphatase 3 are the primary enzymes for C1P de novo anabolism and catabolism, respectively, and exploiting their regulation can modulate wound healing.** Observing loss of acid sphingomyelinase (ASM) may uncover how much Cer derives from the de novo pathway, phosphorylated downstream to yield C1P, as well as exploiting this enzymes effects on eicosanoid synthesis. Although it is proposed CerS5 is the prevalent isoform in lung epithelia[5], preliminary data suggests loss of CerS1 reveals

widespread losses in eicosanoids, unveiling C18 Cer as the possible chain length preferred by CERK. There are three isoforms of lipid phosphate phosphatases (LPPs), however, their regulation is not well understood. It has been revealed that LPP3 is structurally different from the other isoforms, found in a uniform distribution across cell types, and is involved within post-Golgi trafficking[6]. This suggests its larger role in sphingolipid metabolism. This study addresses our hypothesis by i) *in vitro* identification of anabolism and catabolism of C1P in lung epithelial cells to classify this novel pathway, and ii) *in vitro* analysis aims to explore amount of C1P generated from de novo sphingolipid synthesis.

By selective knockdown of each isoform of CerS, we expect to find the primary isoform responsible for C1P metabolism. Anabolism of C1P will be evaluated by eicosanoid analysis in absence LPP isoforms. C1P generation can occur by an S1P acylase[7], it is suggested isoforms of CerS may harbor this activity. By comparing loss of CerS1 to ASM in lung epithelial cells, it can be identified which pathway C18 Cer commonly derives from, thereby revealing amount of C1P present from limiting ceramide synthesis to sphingomyelin or de novo specific utilizing eicosanoid analysis. ASM and NPC1 are similar in function[8], we aim to determine whether NPC1 plays a role in C1P metabolism. Lastly, exploring the function of SM derived C1P and de novo derived C1P to compare how wound healing differs between these distinct pathways. This is significant because exploiting the metabolism of C1P can help identify new targets for therapeutics, as well as validating this enigmatic yet novel pathway.

CHAPTER ONE: INTRODUCTION

Sphingolipid Metabolism

In 1884, J.L.W. Thudichum discovered an elusive class of lipids within brain tissue, coined the term “sphingolipids” after the enigmatic nature of the Sphinx[9]. Isoforms of ceramide synthases (CerS), each with distinct substrate specificity for fatty acyl chain lengths, yield chain lengths of Cer from precursor sphingolipids. Cer is synthesized in the endoplasmic reticulum (ER) and moved to the Golgi actively by ceramide transport protein (CERT) or passively by vesicular trafficking[10]. Ceramide kinase (CERK), associated with the cytosolic trans-Golgi network (TGN), phosphorylates Cer to yield C1P. It is unknown which chain length of Cer is preferred by CERT to be processed downstream by CERK, or which chain length of Cer is preferred to be processed downstream by CERK. C1P anabolism and catabolism is also not well understood, and the amount of C1P which derives from the de novo pathway **(Fig.1)** is unknown[11]. This study aims to address these gaps in knowledge in order to provide a better understanding of C1P metabolism, and how this pathway can be manipulated for inflammation and wound healing.

CerS yields Cer by acylation of precursor sphingolipids. Unlike other CerS isoforms **(Table.1)**, CerS1 has unique regulation, and is known to translocate from the ER to the Golgi in response to stress. Previous studies reveal that in response to variety of different stressors, such as drug treatment and radiation, CerS1 is cleaved by protein kinase C (PKC) in order to translocate to the Golgi[12].

We hypothesize inflammation causes this stress induced translocation as well, causing this isoform to synthesize robust amount of C18 Cer to yield C1P downstream to accelerate production of eicosanoids. C18 Cer has been shown to have diverse function in stress response, as seen in cancer in chemotherapeutic drug response[13-14], Other common chain lengths of Cer function in cell death, such as pro-apoptotic C16 Cer yielded by both CerS5 and CerS6[15]. CerS5 is detected as the main isoform within lung epithelia[5], whereas CerS1 is found throughout cell types in lower levels, but more prominent in neurons[16]. Although not as abundant as CerS5, preliminary data details absence of CerS1 mediated C18 C1P reveals drastic changes in eicosanoid synthesis **(Fig.2)**, hinting at the different function this isoform has.

Preliminary data reveals CerS1 inhibition shifts the eicosanoid profile within A549 nonsmall cell lung cancer (NSCLC) cells **(Fig.2)**. This suggests C18-20 Cer, yielded exclusively by CerS1, may be the substrate favored by CERT to be phosphorylated by CERK to yield C1P. Additionally, CerS1 is structurally different from the other isoforms due to the absence of a hox-like domain. Homeobox proteins with this domain function as transcription factors in development[17], however, these are missing residues essential for DNA binding[18]; elucidating a different underlying function for CerS1. It is suggested lipid phosphate phosphatases (LPPs) cause the regression of C1P to Cer after eicosanoid synthesis. LPP3 cycles between the ER and Golgi, alluding to its role in lipid trafficking, but it is unknown how it regulates lipid metabolism[19]. The role of LPP1 is also explored, due to its proven role in degradation of LPA, which functions in angiogenesis[20]. The cell requires a delicate balance of sphingolipids, to prevent accumulation of sphingomyelin (SM), it is broken down to Cer via ASM, yielding Cer from a different pathway: the SM

cycle. It is known that increased C1P levels can inhibit ASM activity by Orm sensors[21]. Additionally, Niemann Pick Type C protein-1 (NPC1) is known to be similar in function to ASM[22], absence of either results in lysosomal storage disease[23]. It is unknown whether NPC1 plays a role in C1P metabolism. Modulating this relationship, we can assess the total amount of C1P which derives from the de novo pathway.

Ceramide 1-Phosphate

C1P activity is abated by ASM or breakdown by LPPs. Absence of ASM prevents formation of ceramides, resulting in inhibition of apoptosis by exacerbated C1P activity[24]. Inhibition of ASM may provide insight on the amount of C1P derived from the de novo pathway exclusively, further detailing the biological function of distinct chain lengths of C1P. LPPs are expressed on internal membranes and dephosphorylate a variety of lipid phosphates, including C1P. Each isoform has their own distinct function, however the primary isoform which yields C1P is unknown. Unlike other isoforms, LPP3 has an arginine-glycine-aspartate (RGD) recognition motif, which enables interaction with integrins at membranes[25]. LPP3 has been observed to traffic between the Golgi and ER, which elucidates its role in catabolism of bioactive inflammatory lipids[19]. Additionally, NPC1 functions in lipid trafficking, inhibition results in a phenotype similar to lack of ASM due to accumulation of precursor lipids and subsequent ablation of lipids within ER and Golgi[26]. Delving into this protein may provide insight on how this lysosomal storage disease affects C1P metabolism, and if this is consistent with ASM deficiency, how modification of these metabolites may serve to improve quality of life with those suffering from this rare, genetic disorder[27].

Eicosanoid Metabolism

Yearly, 1.7 million Americans develop sepsis, and 1 in 3 patients who die in a hospital is due to sepsis[28]. Sepsis is the result of an adverse host response to infection, resulting in the immune system working in overdrive. Eicosanoids are a bioactive class of lipids which function as inflammatory mediators, beginning with the initial rate limiting step of arachidonic acid (AA) **(Fig.3)** formation by activation of group IVA cytosolic PLA_2 ($cPLA_{2\alpha}$)[29].Previous work in our lab reveals that eicosanoid biosynthesis is modulated by C1P (ceramide 1-phosphate), which directly activates $cPLA_{2\alpha}$ by interacting with the C2/calcium dependent lipid binding (CaLB) domain, thereby decreasing the dissociation rate of this enzyme from phosphatidylcholine (PC) rich membranes[11].

Inflammatory agonists, such as ATP and cytokines, cause activation and subsequent translocation of cPLA2α by association with membranes in a Ca2+ dependent manner by C2/CALB domain[30]. The mechanism of eicosanoid synthesis starts with arachidonic acid (AA), the rate limiting step[31]. Previous work in our laboratory has revealed C1P as a cofactor in eicosanoid synthesis by activating cPLA2α **(Fig.4)** by using naturally occurring C16 and C18:1 C1P[30]. However, is not well studied if different chain lengths of C1P have distinct biological effects. Currently, only one drug on the market exploits this pathway to produce an anti-inflammatory response: aspirin. By selective acetylation of cyclooxygenase-1 (COX-1) at Ser-530, prostaglandin synthesis can be inhibited[32]. Recent studies suggest aspirin binding with cPLA2α causes this anti-inflammatory effect[33], elucidating potential upstream targets to combat inflammation. Delving into the specific enzymes responsible for anabolism and catabolism of C1P may

provide insight on clinical targets to impede sepsis and modulate the wound healing response.

Clinical Relevance

In recent years, the field of lipidomics has flourished, unearthing their effects on inflammation, cancer, pre-eclampsia, neurological diseases and sepsis[34]. Sepsis can occur from viral, fungal, or bacterial infection. In 2017, it was found that almost 20% of all global deaths were sepsis-related[35]. There is no specific treatment, but rather management of symptoms, infection, and organ support[36]. Sepsis also places heavy burden on patient expenses and hospital resources, when comparing admission of all other disease states, the price of managing sepsis in U.S hospitals is the highest. Additionally, the average length of stay for septic patients has a 75% greater duration than most conditions[36]. Methods to identify early biomarkers of sepsis, or by targeting enzymes involved in creation of inflammatory mediators, may prove useful for reducing the burden and severity of sepsis in the U.S.

Hypothesis

Inflammatory C1P anabolism occurs from CerS1 while catabolism occurs due to LPP3 specifically and modulating these upstream enzymes may change the rate of wound healing. The role of ASM serves to compensate for lack of CerS, and in this enzyme's absence, which reveals the amount of C1P from the de novo pathway.

Significance

Successful completion of SAs will improve our understanding of C1P metabolism, specifically how and where C1P is created and its fate postproduction of eicosanoids by catabolic enzymes. Exploring the specific function and relationship between these enzymes may reveal potential therapeutic targets for combatting sepsis. Wound healing rates can be potentially altered by modulating upstream enzymes of C1P. This will benefit the quickly growing field of lipidomics, delineating the mechanism and role of C1P in wound healing and inflammation. We address our hypothesis using in vitro analysis with two distinct lung epithelial cells, A549s and HBEC3-KT, to study C1P metabolism and effects on inflammation. Cells from the airway epithelium play a large roll in innate immunity, inflammation and tissue remodeling[37], which makes them reliable models for studying C1P metabolism in inflammation. Exploring C1P metabolism may reveal potent, upstream targets for inflammatory therapeutics, as well as expanding the growing field of lipidomics.

Research Aims

R1) Identify the enzymes and metabolic processes in which anabolism and catabolism of C1P occurs in vitro.

R2) In vitro analysis to determine the amount of C1P from the de novo pathway

Figures

Table 1: Isoforms of ceramide synthase
Substrate specificity for each isoform of ceramide synthase (CerS), which yields corresponding chain lengths of ceramide (Cer).

Ceramide synthase	Acyl chain length
CerS1	C18
CerS2	C22-C26
CerS3	C22-C26
CerS4	C18-C20
CerS5	C16
CerS6	C14-C16

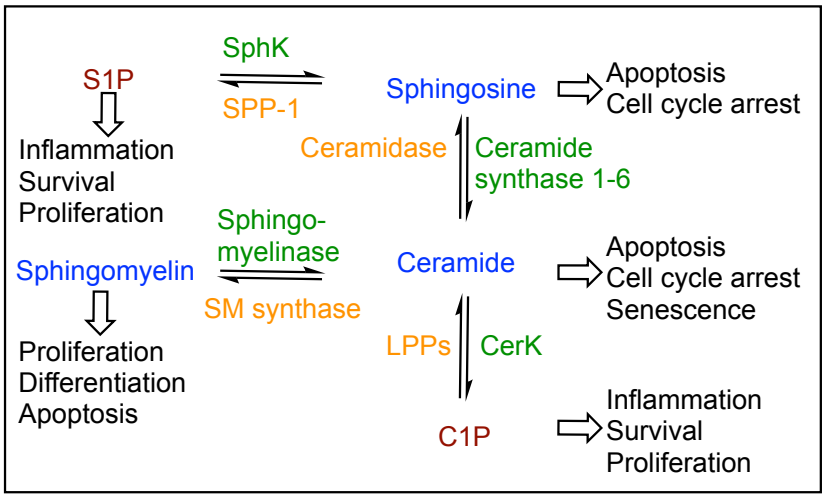

Figure 1 De novo pathway of ceramide formation
General characteristics for each metabolite are outlined. Enzymes responsible for anabolism and catabolism are highlighted in orange and green, respectively. Pro-apoptotic lipids are indicated in blue while pro-inflammatory lipids are red.

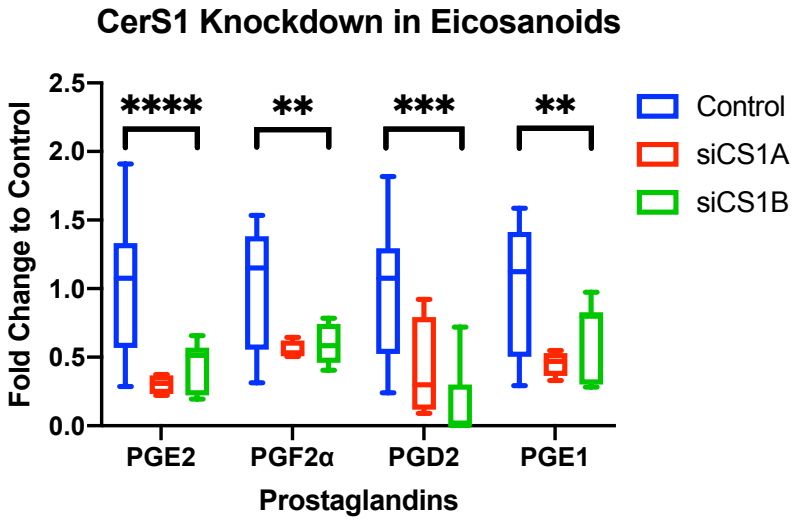

Figure 2 Preliminary data
Upon loss of CerS via two different targeting siRNAs, eicosanoid analysis of cell media in A549 cells reveal drastic changes in prostaglandin synthesis, which function as downstream inflammatory mediators (P value ****≤ 0.0001 ***≤ 0.001 **≤ 0.01).

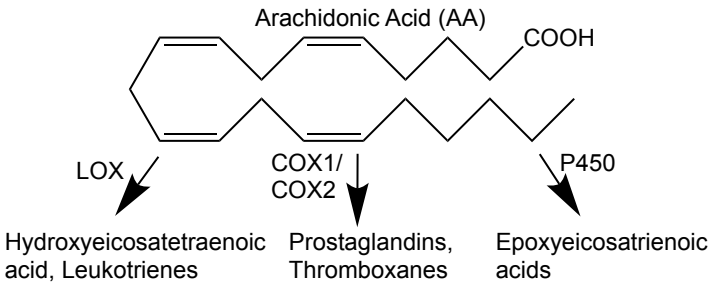

Figure 3 The rate limiting step
Arachidonic acid yields a variety of inflammatory mediators, each play an essential role within the wound healing process.

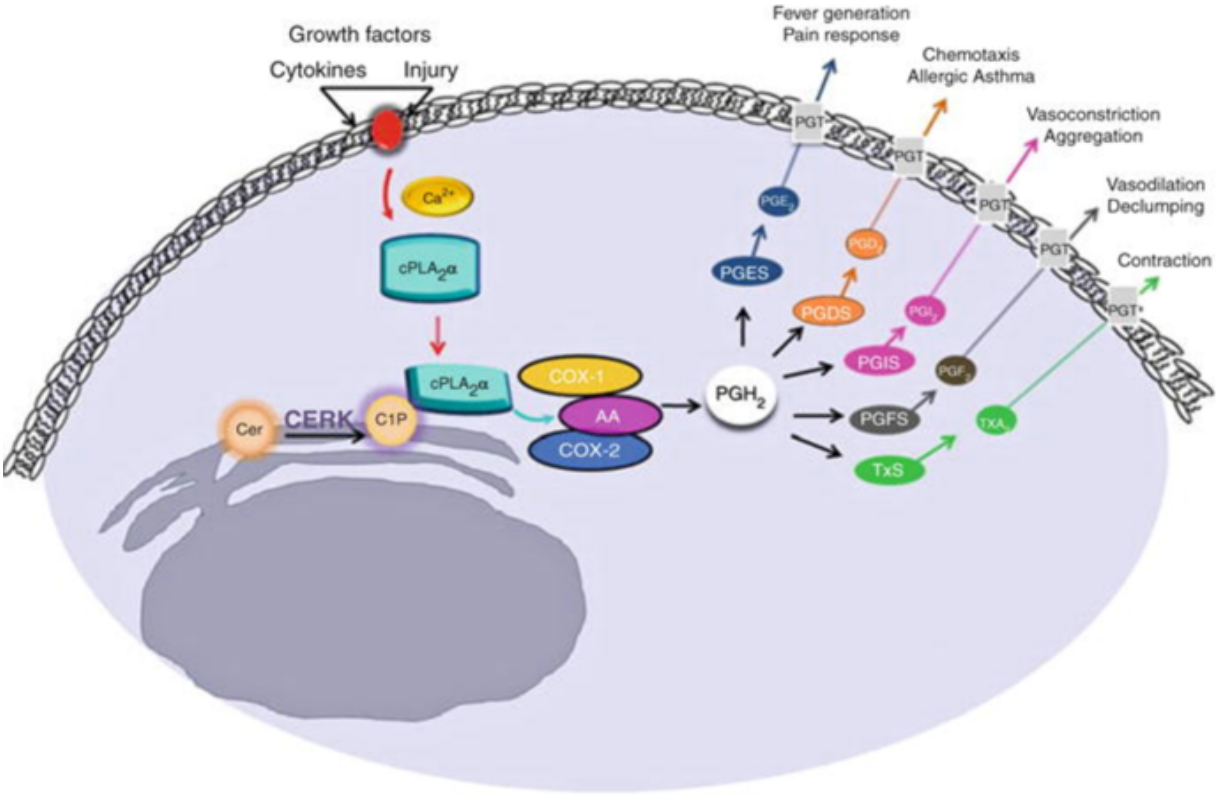

Figure 4 C1P and cPLA2α interaction

The relationship between C1P and cPLA2α serves as the crucial link in eicosanoid synthesis. Hydrolysis of PC by cPLA2α produces AA, metabolites of this rate limiting step include prostaglandins, which are responsible for a variety of inflammatory responses. (Adapted from Chalfant Lab – Hoeferlin et al., 2017)

CHAPTER TWO: ANABOLISM AND CATABOLISM OF C1P

Abstract

Six isoforms of ceramide synthase (CerS) yields ceramide (Cer) from precursor sphingolipids. Preliminary studies reveal some isoforms have more of an effect on sphingolipid and eicosanoid metabolism than others. The differences in these effects are due to the chain lengths of Cer each isoform yields **(Table.1)**, as well as the tissue types these isoforms are prominently found in. For example, CerS3 yields very long chain lengths of Cer in low levels, specific to tissues in the testes and epidermis[38]. In absence of CerS1 specifically, which yields C18 Cer, we notice large changes in lipid metabolism in preliminary data; specifically, absence of the inflammatory mediators: prostaglandins **(Fig.2)**. This provides insight that C1P primarily arises from the de novo pathway of Cer formation, which will be explored further in the next chapter. Catabolism of C1P is largely undiscovered, it is suggested isoforms of LPP are responsible for this, LPP3 is a potential candidate due to its role in cellular trafficking[39]. By analyzing protein levels of each LPP isoform in overabundance of precursor substrate C1P, we can uncover which isoform is primarily responsible for conversion of C1P back to Cer. By distinguishing which isoform of LPP is responsible, we can explore potential therapeutics for sepsis, target its expression to modulate wound healing and inflammation.

The goal of this chapter is to test the hypothesis that **de novo creation of C1P derives from formation of ceramide by ceramide synthase 1, and C1P catabolism**

is mediated by lipid phosphate phosphatase 3 specifically. To address this hypothesis, we use *in vitro* analysis of both A549s and HBEC3-KTs to determine the novel mechanisms of C1P metabolism. Inflammation and proliferation are characteristic for C1P, we compare and contrast these lung epithelial cell lines due to their role in the immune and inflammatory response[40], revealing the effects of the enzymes responsible for catabolism and anabolism of this inflammatory mediator. Additionally, use of HBEC3-KTs establish baseline levels of sphingolipid and eicosanoid metabolism, we may observe differences in lipid metabolism due to the nature of lung cancer cells.

Introduction

In order to determine if CerS1 yields the substrate of Cer preferred by CERK to yield C1P, siRNA knockdown of each isoform will be performed. Absence of each individual isoform reveals different results depending upon the chain lengths yielded. Protein analysis by western blotting with corresponding antibodies to each isoform of CerS will be executed to confirm knockdown was successful. Use of non-targeting siRNA as our negative control will provide the underlying level of sphingolipid and eicosanoid expression. Fumonisin B1 (FB1) is a mycotoxin known to inhibit production of Cer[41-42], this drug treatment will serve as our positive control to assess changes when all isoforms are inhibited. By using both A549s and HBEC3-KTs, we can observe these effects in lipid metabolism and inflammation on lung epithelial cells. After harvesting both cell lines with

metabolism, specifically downstream eicosanoids involved in the inflammatory process **(Fig.5)**. Some sphingolipids, such as S1P, are found in low levels throughout the cell[43]. To provide an easier readable format for analysis, this data is converted to fold change to the control. Isoforms downregulated by siRNA knockdown and drug treatments will reveal absence of corresponding chain lengths of Cer, as well as provide insight on how the cell compensates for this loss by elevating other levels of sphingolipids and eicosanoids.

There are three isoforms of LPP[44], but which isoform that converts C1P to Cer specifically is unknown **(Fig.6)**. By observing these metabolites, we can deduce which isoform is primarily responsible for yielding Cer by examining drastic decreases in our isoform of interest when its substrate is missing. When viewing analysis of eicosanoids, we anticipate the effects of unregulated generation of C1P, an increase in eicosanoid synthesis due to our candidate LPP3 due to an increase in substrate C1P levels.

S1P is a known substrate for C1P generation, however the identity of this enzyme is unknown[45-46]. This will be assessed by harvesting cells treated with CerS inhibitor FB1 (Cayman Chemical). Our control will be cells treated with DMSO, the solvent used to dissolve FB1. In order to quantify the amount of C1P, cells will be harvested and media conserved for eicosanoid analysis utilizing aforementioned tandem HPLC/MS. Chain lengths of C1P yielded by other isoforms in absence of CerS1 will be assessed by integrating spectrograph lipid data (pmol/100,000 cells). By observing C1P levels in cells with CerS inhibition, we can conclude whether these synthases can yield C1P from S1P, and if this is specific to a particular isoform.

Materials and Methods

Cancer Cell Lines and Media

The non-small cell lung cancer (NSCLC) cell line A459 and immortalized human bronchial epithelial primary cells (HBEC3-KT) infected with human telomerase (hTERT) and cyclin dependent kinase 4 (CDK4) (purchased from American Type Culture Collection, ATCC) **(Appendix A)** were cultured in DMEM (A549; Gibco) or Airway Epithelial Cell Basal Medium and Bronchial Epithelial Cell Growth Kit (HBEC3-KT; Thermofisher). DMEM was supplemented with 10% fetal bovine serum (FBS, Gibco) and 1% penicillin/streptomycin (Gibco). Cell lines were maintained in an incubator at 37°C with 95% air and 5% CO2. Cells were nourished at 80% confluency. For each cell line, subsequent analysis was performed within the first 10 passages. Prior to harvesting cells for lipid and protein analysis, all samples were rested for 24 hours in DMEM (Gibco) with 2% serum and 1% antibiotic to reduce the adverse effects of serum growth factors on eicosanoid and sphingolipid production.

Protein Extraction and Western Blot Analysis

Cells were harvested on ice in PBS (Gibco), spun down in a microcentrifuge (Sorvall Legend Micro 21R Centrifuge, Thermofisher) at 3.5 RPM for 5 minutes to remove supernatant. Prior to sonication, samples were resuspended in CelLytic lysis regent with 1% protease phosphatase inhibitor (Sigma Aldrich). To decrease viscosity, samples were spun down again. Amount of protein was then quantified using Bradford Protein Assay according to manufacturer's instruction (Bio-Rad).

Samples were prepared for western blot analysis by addition of equal amounts 2x laemmli buffer with 5% beta-mercaptoethanol (Bio-Rad). Samples were then heated at 100 C for 5 minutes, then 15 ug of protein was run on 10% polyacrylamide gels (Bio-Rad) using a PowerPac (Bio-Rad) at 30 mV for 15 minutes and 100 mV for 1.5 hours. Protein was transferred to PVDF membranes using a wet transfer technique according the manufacturer's instructions (Bio-Rad).

Membranes were blocked in 3% nonfat milk in TBST (Bio-Rad) for 1 hour, then blocked overnight at 4 C in primary antibodies outlined in the *Reagents and Antibodies* section. Milk was discarded and membranes were washed in TBST for an hour in 15-minute intervals, then blocked in anti-host secondary antibodies for an additional hour. After discarding milk, a two-hour TBST wash step took place, then membranes were imaged using chemiluminescent HRP substrates (Bio-Rad). Images of protein blots were saved and quantified on Image Lab Software (Bio-Rad), gene silencing was assessed after normalizing protein expression to loading controls.

RNAi Transfection

Lung epithelial cell lines were seeded at confluency of 1.5×10^5 cells per well within 6-well plates. 24 hours later, cells were transfected with RNAi (non-targeting control or gene silencing siRNA), with premade sequences. Before addition to cells, RNAi reagents were rested in Dharmafect 2 (Horizon Discovery) for 20 minutes. A stock concentration of 100 uM siRNA in water was diluted to 25nM final concentration in 2% serum media.

Drug Treatment

Seeded at 3.0 x 10^5 cells per well in a 6-well plate, lung epithelial cells were grown over a 24 hour period. Drug treatment by 50 uM FB1 (Cayman Chemical) or 70 uM desipramine hydrochloride (Sigma Aldrich) were applied to cells in 2% serum media. Controls included cells treated with solvent drug was resuspended in, DMSO (Dharmacon). After appropriate drug treatment duration, cells were harvested, and media was conserved for successive analysis

Sphingolipid Extraction

In 6-well plates, lung epithelial cells were harvested in PBS (Gibco), centrifuged and supernatant was removed. Before extraction, samples were temporarily stored at -80 C. Utilizing monophase bligh dry extraction, cell pellets were vortexed in LC/MS grade water optima (Thermofisher). Internal standard was added to each sample vial, vortexed and sonicated to break apart pellets. 2:1 ratio of LC/MS grade methanol to chloroform (Thermofisher) was added, cells were sonicated individually and placed in a 48 C water bath shaker (Precision SWB15, Thermofisher) for 6 hours at 30 RPM. Samples were sonicated prior to centrifugation for 10 min at 4,000 RPM. Organic solvent was transferred to a glass vial and dried down for 2.5 hours (Savant SPD2010 Speedvac Concentrator, Thermofisher). 500uL methanol was added to each sample, sonicated the spun down at 4,000 RPM for 1 minute. Aqueous layer was then transferred to autosampler vials for HPLC-MS analysis

Eicosanoid Extraction

Media from 6-well plates were aliquoted and temporarily saved at -80 C for subsequent analysis using solid phase affinity chromatography. Media was thawed and each sample was prepped for extraction by addition of 100uL methanol, 5uL acetic acid, and 20uL internal standard per mL of media (LC/MS grade, Thermofisher). In a vacuum manifold filter chamber (Agilent Technologies), filter columns were washed by adding 2 mL of methanol, then 2 mL of water (Thermofisher), then sample. To collect misnomer lipids, remaining sample was resuspended in 5% methanol and applied to filter columns. Wash tubes (Falcon) were discarded, and eicosanoids were collected by applied 2 mL isopropanol (Thermofisher). Samples were then dried down for 5 hours (Savant SPD2010 Speedvac Concentrator, Thermofisher), then redissolved in 50:50 ethanol and water (LC/MS grade, Thermofisher). After vortexing, samples were centrifuged at 5,000 RPM for 15 minutes, then transferred to autosampler vials for HPLC-MS analysis.

HPLC-MS

Using tandem High-Performance Lipid Chromatography and Mass Spectometry[47] and a C18 column (Kinetex), a 14 minute reverse phase LC method was utilized for eicosanoid separation at 50 C with a 200 uL/minute flow rate. Prior to the sample run, column equilibration was accomplished for 10 minutes with 100% Solvent A, a 40:60:0.02 ratio of acetonitrile, water and formic acid (Thermofischer). 10 uL of each sample was injected per run. Within the first minute, 100% Solvent A was used for elution. In a linear gradient, amount of Solvent B- composed of 50:50:0.02 acetonitrile, isopropanol, and formic acid- was increased in a temporal manner by increments of 15%. Towards the end

of the run, Solvent B was eluted at 100%. Eicosanoid analytes were quantified by tandem quadrupole mass spectrometer (SciEx Selection). In negative-ion mode, multiple-reaction monitoring of eicosanoids was accomplished using parent ions, which were then fragmented in the collision cell, which yielded product ions of our analytes of interest. These quantitative results were assessed using Quantitation Wizard (Analyst Software, SciEx), then exported for normalization and statistical analysis on Excel (Microsoft Office).

Statistical Analysis

Statistically significant data is defined by a p-value equal to or less than 0.05, each value outlined as mean ± standard deviation (SD). Biostatistics analysis utilized either R or GraphPad Prism 8 (GraphPad Prism Software). For comparisons between multiple samples, ANOVA with Tukey post-test were used for subsequent analysis.

Reagent and Antibodies

To assess gene silencing, SMARTpool siRNA for CerS1, CerS6, LPP1 and LPP3 (Dharmacon) was utilized. For specific isoform functional studies, single variants within specific regions need to be targeted utilizing individual siRNA targeting the open reading frame (ORF) for CerS1 (Sigma Aldrich), CerS6 (ON TARGETplus, Dharmacon), LPP1 (FlexiTube Gene Solution, Qiagen) and LPP3 (ON TARGETplus, Dharmacon). Two out of four individual siRNAs within pool were selected for comparison, both achieving a decrease in at least 50% protein expression.

Western blots were performed utilizing the following antibodies: Our loading control was assessed using anti beta-actin antibody (1:2000, Cell Signaling). To validate gene

silencing, antibodies for CerS6 (1:1000, Santa Cruz), CerS1 (1:500, abcam), LPP1 (1:1000, PPAP2A Polyclonal from Invitrogen), and LPP3 (1:500, VCIP Monoclonal from Thermofischer) were employed. Anti-rabbit and anti-mouse secondary antibodies (1:5000, Cell Signaling) were utilized to reduce appearance of nonspecific proteins.

Results

Anabolism of C1P

The primary constituents involved in anabolism and catabolism of C1P will be unveiled by gene silencing, protein analysis, and identification of analytes via tandem HPLC-MS. To discern which isoform of CerS is responsible for creation of C1P, downregulation of each isoform is required to observe how this impacts sphingolipids and eicosanoids **(Fig.7)**. FB1 has been studied immensely, known to inhibit creation of Cer. This mycotoxin will serve as the baseline for downregulation of all CerS isoforms. Although C14 and C16 Cer are prominent in the cell, we hypothesize C18 Cer plays a larger role in C1P anabolism due to its roles in stress response[48-49], which is yielded by CerS1 **(Fig.8)**. We expect that, with absence of CerS1, we will observe absence in C1P mediated characteristics, such as proliferation and inflammation. 5-HETE is an eicosanoid and known inflammatory agonist, loss of CerS1 specifically should reveal widespread loss of this particular eicosanoid, thereby confirming our hypothesis that CerS1 is the enzyme responsible for anabolism of C1P **(Fig.9)**. This is significant because biomarkers and potential therapeutic targets up stream of C1P may be evaluated for clinical use. The importance of CerS1 is substantiated by analysis of CerS6, another isoform which yields shorter chain lengths of Cer. We observe an accumulation of de novo precursor lipid Sa

(Fig.10), and compensation phenemona among the other isoforms by increased long chain lengths of Cer. The effects of phosphorylating these long chain lengths portray a loss in anti- and pro-inflammatory mediators, including AA, DHA and EPA **(Fig.11)**. Prostaglandin synthesis is perturbed, absence of CerS6 has more of an effect on downstream COX eicosanoids than absence of other candidate isoform CerS1, portraying the importance of C16 Cer in the de novo pathway of C1P generation.

Catabolism of C1P

It is suggested catabolism of C1P mediated by LPP3 specifically can be confirmed if eicosanoid production is levels increased in absence of this metabolite **(Fig.12)**. This details the mechanisms the cell utilizes to maintain the delicate balance of these lipids, thereby mediating the inflammatory response. Because C1P is prominent in proliferating cells, we expect to see exacerbated differences in metabolism in cancer cells in comparison to noncancerous lung epithelial cells. Without LPP3, C1P synthesis is unregulated, resulting in drastic increases of prostaglandin synthesis and eicosanoids downstream of LOX. Insight into the enigmatic mechanisms of C1P metabolism will reveal how it is created and recycled in the cell, as well as subsequent effects on eicosanoid production **(Fig.13)**. This also elucidates potential targets for drugs combatting inflammation and sepsis. Currently on the market as the highest grossing medication, aspirin, targets cyclooxygenases (COX1/COX2) to alleviate headaches[32-33]. This is a downstream constituent of C1P mediated eicosanoid metabolism. However, insight into the creation of this pro inflammatory mediator C1P may reveal new upstream drug targets in order to combat inflammation and sepsis.

S1P as a substrate

Studies have found an unidentified acylase responsible for yielding C1P using S1P as a substrate[50]. By analyzing S1P levels in lung epithelial cells in absence of CerS isoforms, it can be determined if this is a substrate for CerS mediated C1P synthesis. In cells treated with FB1 **(Fig.14)**, we expect endogenous S1P levels to dip slightly, as SPP-1 can convert S1P to precursor sphingosine[51]. However, with the absence of CerS, we expect to see a buildup of precursor lipids due to lack of Cer generation **(Fig.15)**. C1P levels should remain low due to absence of CerS, but in absence of only one isoform, other isoforms of CerS may compensate for this lack and yield their respective chain lengths of Cer to be phosphorylated downstream[52]. We hypothesize, in absence of isoforms of CerS, S1P levels should increase, due to lack of enzymes to yield C1P. Lack of C1P should reveal drastic changes in eicosanoid production, due to lack of AA synthesis[53] **(Fig.16)**. As compensation amongst other enzymes is common within lipid synthesis, some eicosanoids may be elevated in attempt to maintain balance within the cell.

Discussion

In absence of CerS6, it is observed other isoforms attempt to compensate for this loss by yielding drastic amounts of their respective chain lengths of Cer. If this happens and we see no changes in sphingolipids and eicosanoids, we can determine what effects are taking place by viewing mRNA levels of the other isoforms of CerS. This new approach would explore the compensation phenomena among CerS isoforms by observing mRNA levels when CerS1 is downregulated in the cell, however, limitations include availability of primers for each isoform of CerS.

LPPs play an essential role in the catabolism of C1P[54]. Without LPP3, eicosanoid analysis unveiled a drastic increase in prostaglandins and other inflammatory mediators. LPP3 is the proposed phosphatase isoform responsible for degradation of C1P, and without its activity, eicosanoid production persists in an unregulated fashion.

S1P may serve as a potential substrate for CerS mediated C1P synthesis[55-56], however, results reveal a decrease in S1P levels. This could be due to activity of sphingosine kinase (SphK), as the cell attempts to compensate for lack Cer generation by accumulation of So. Perhaps another enzyme is responsible for acylation of S1P to yield C1P, such as acid sphingomyelinase[57-58].

Figures

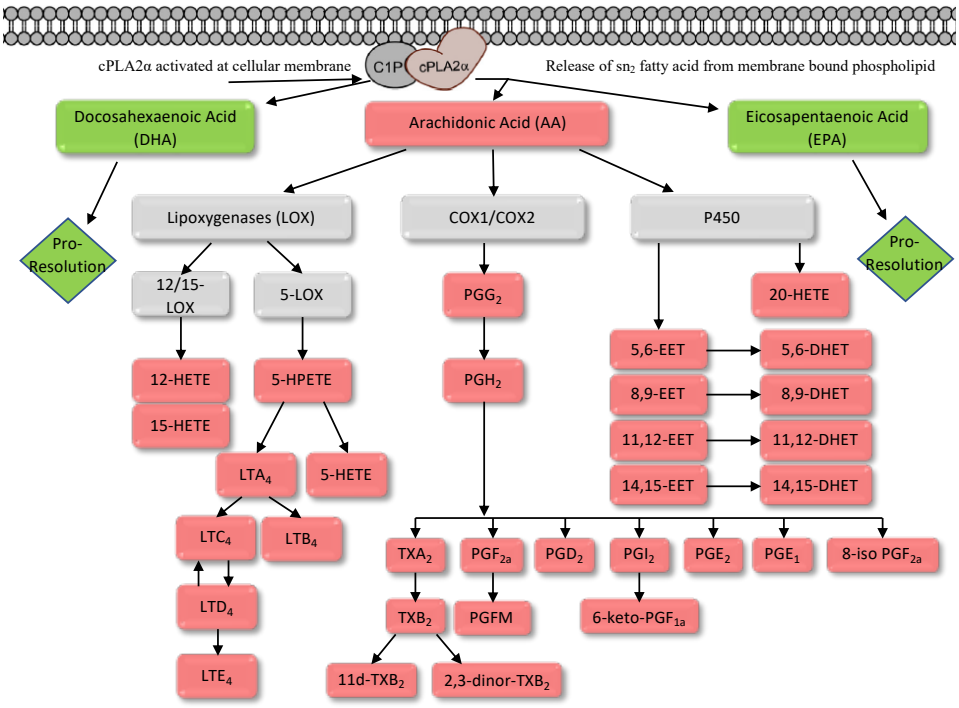

Figure 5 Eicosanoid synthesis
Eicosanoid biosynthesis by C1P-cPLA$_{2\alpha}$ interaction yields pro-inflammatory mediators, indicated in red, downstream of AA. Additionally, this interaction plays an essential role in mitigating the inflammatory response. Downstream of DHA and EPA, anti-inflammatory mediators are indicated in green.

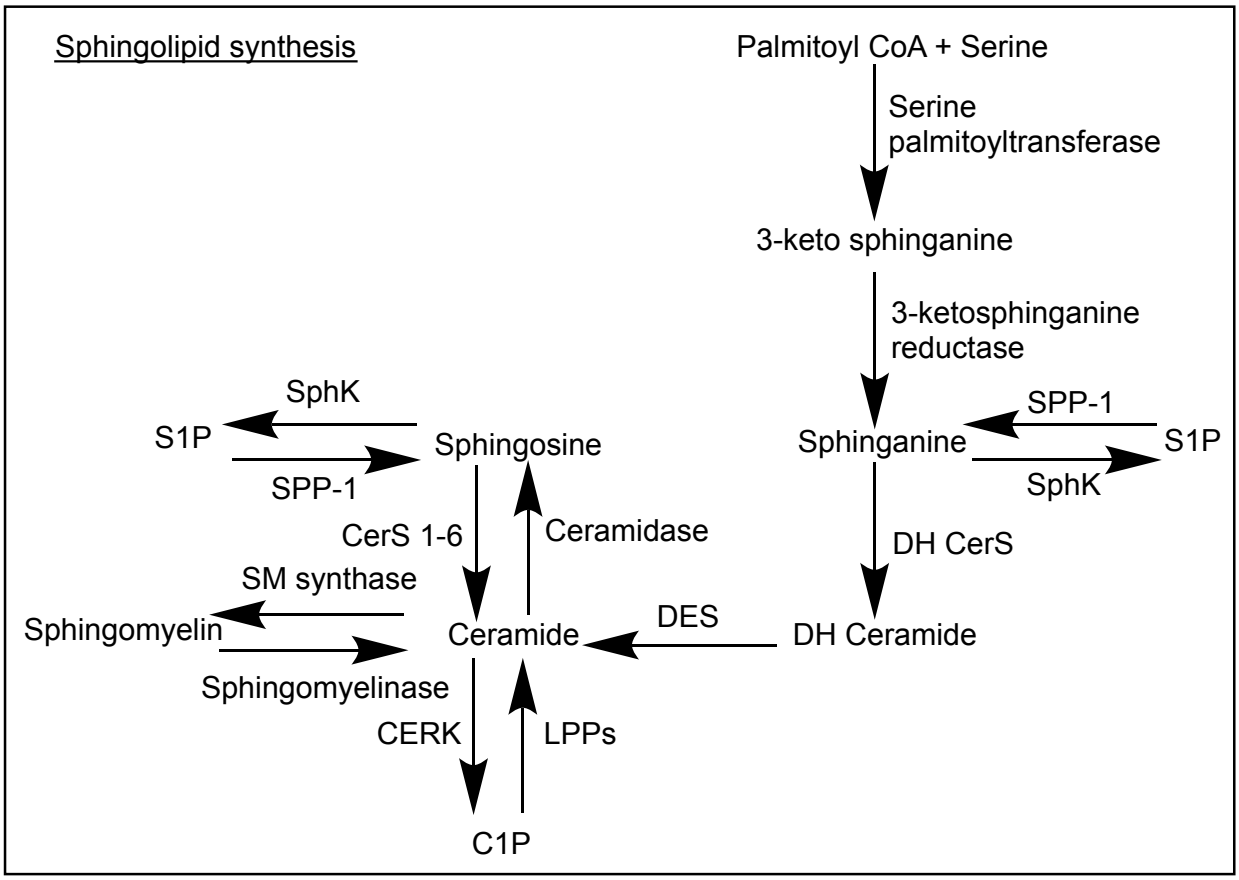

Figure 6 Sphingolipid synthesis
Ceramide is produced in the cell in three ways: de novo pathway by condensation of palmitate derivative palmitoyl coenzyme A (CoA) and serine, salvaged by the re-acylation of sphingosine, or by reduction of dihydro-ceramide (DH-Ceramide) by dihydroceramide desaturase (DES).

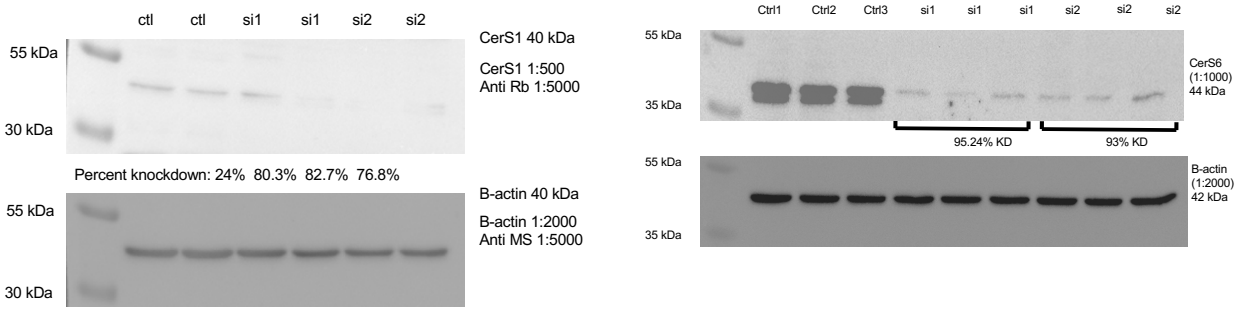

Figure 7 Protein analysis of CerS downregulation
Results confirming decreased protein expression of CerS isoforms essential to C1P synthesis (n=6)

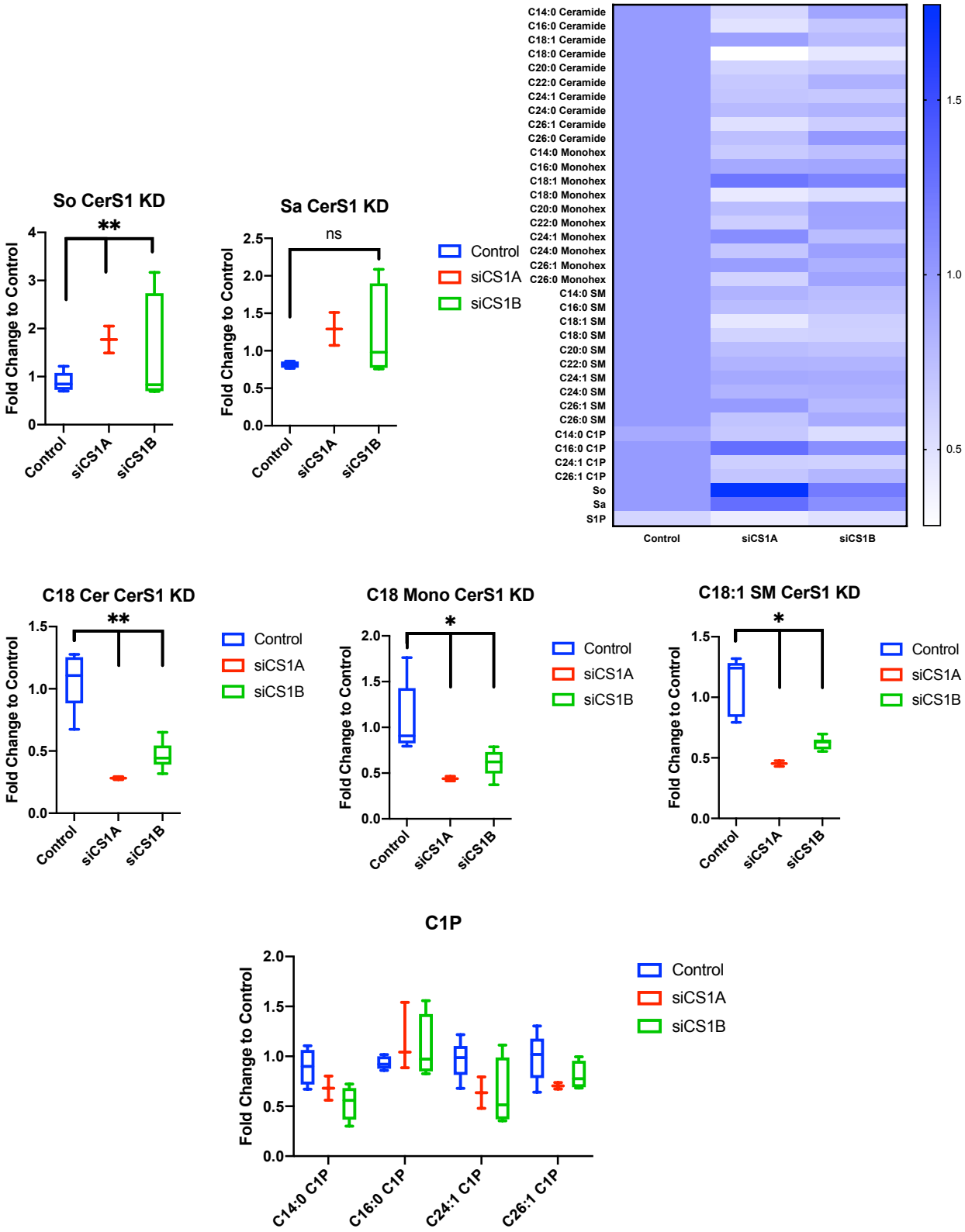

Figure 8 CerS1 sphingolipid analysis
Heatmap illustrating widespread loss of sphingolipids due to absence of CerS1. Statistically significant loss of sphingolipids is elaborated upon using box and whisker plots

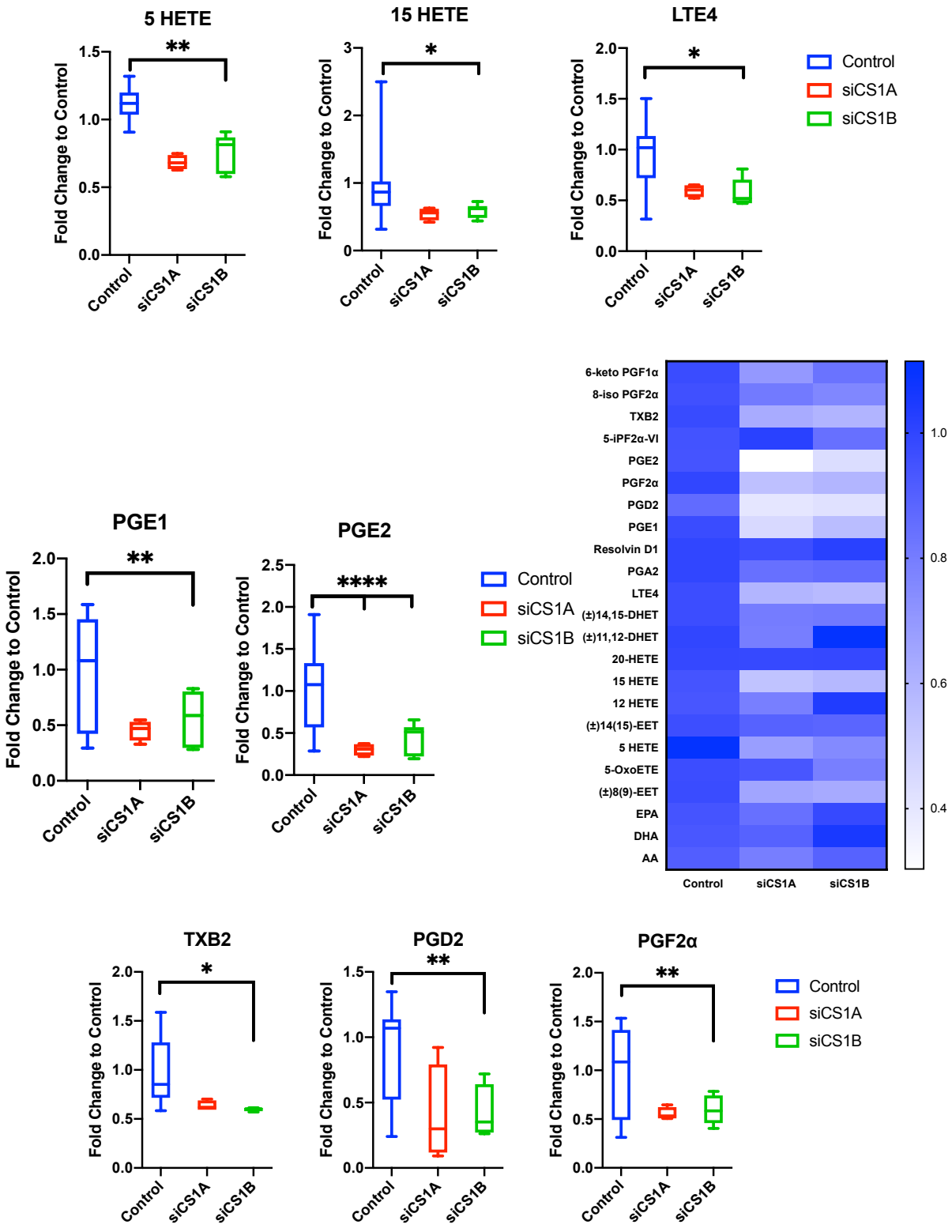

Figure 9 CerS1 eicosanoid analysis
In absence of this particular isoform, downstream inflammatory mediators are mitigated. To compensate for this loss, other isoforms synthesize other eicosanoids to maintain balance in cell metabolism.

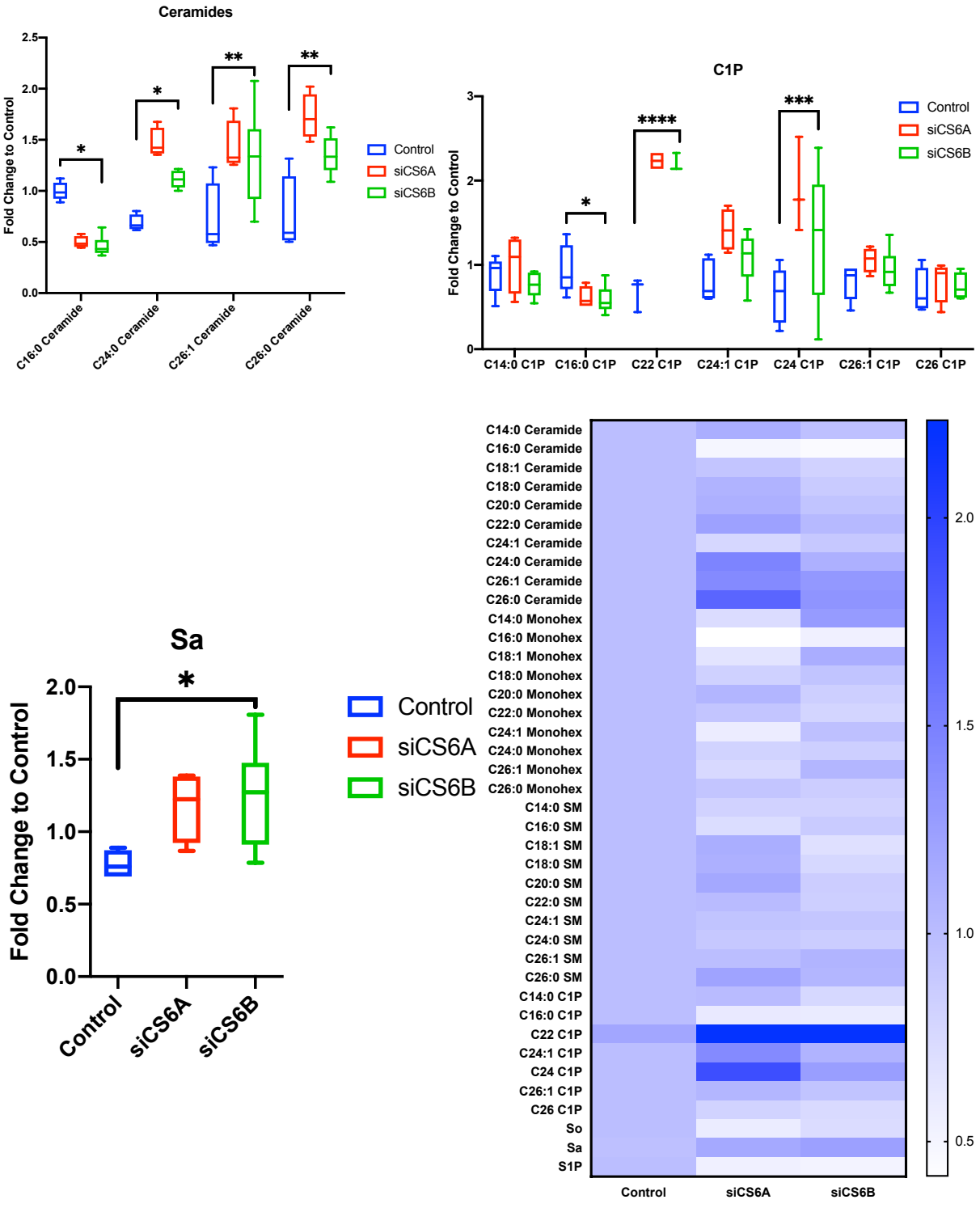

Figure 10 CerS6 sphingolipid analysis
In absence of CerS6, decline in sphingolipid synthesis is portrayed via heatmap. Loss of statistically significant sphingolipids are conveyed by box and whisker plots.

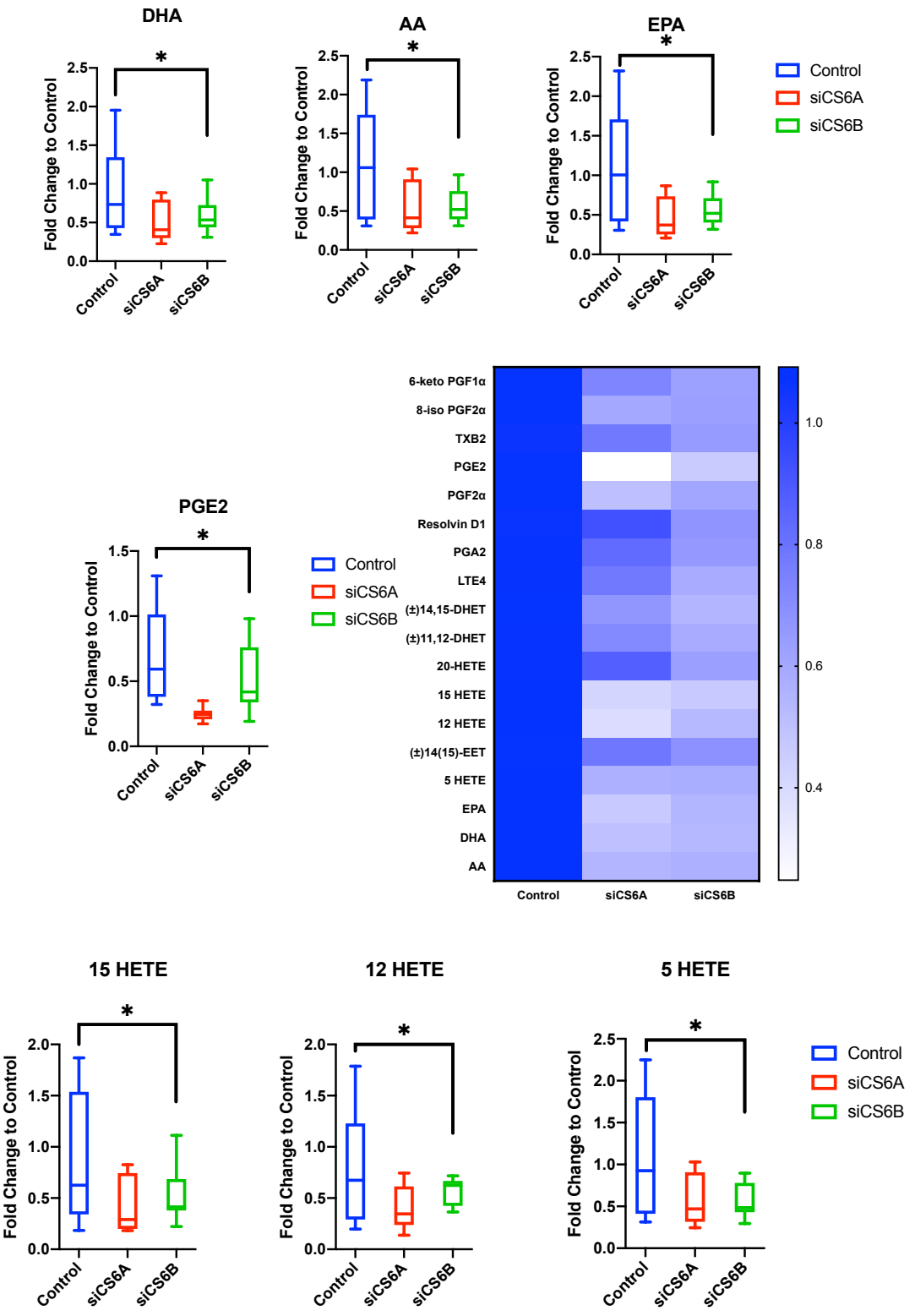

Figure 11 CerS6 eicosanoid analysis
Loss of CerS6 portrays a decrease in inflammatory mediators, general characteristics are shown in a heatmap, specific eicosanoids are elaborated upon by box and whisker plots.

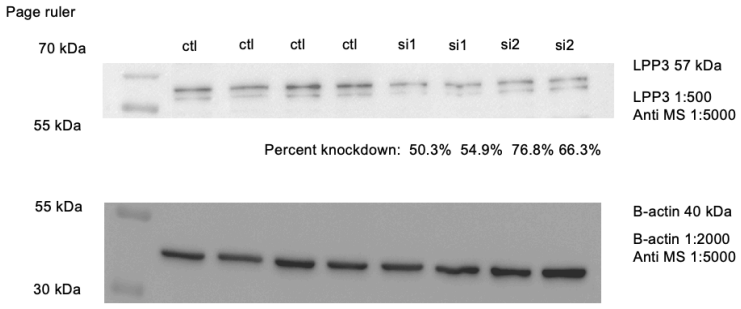

Figure 12 LPP3 protein analysis
Two different individual siRNAs revealed loss of LPP3 expression by over 50%.

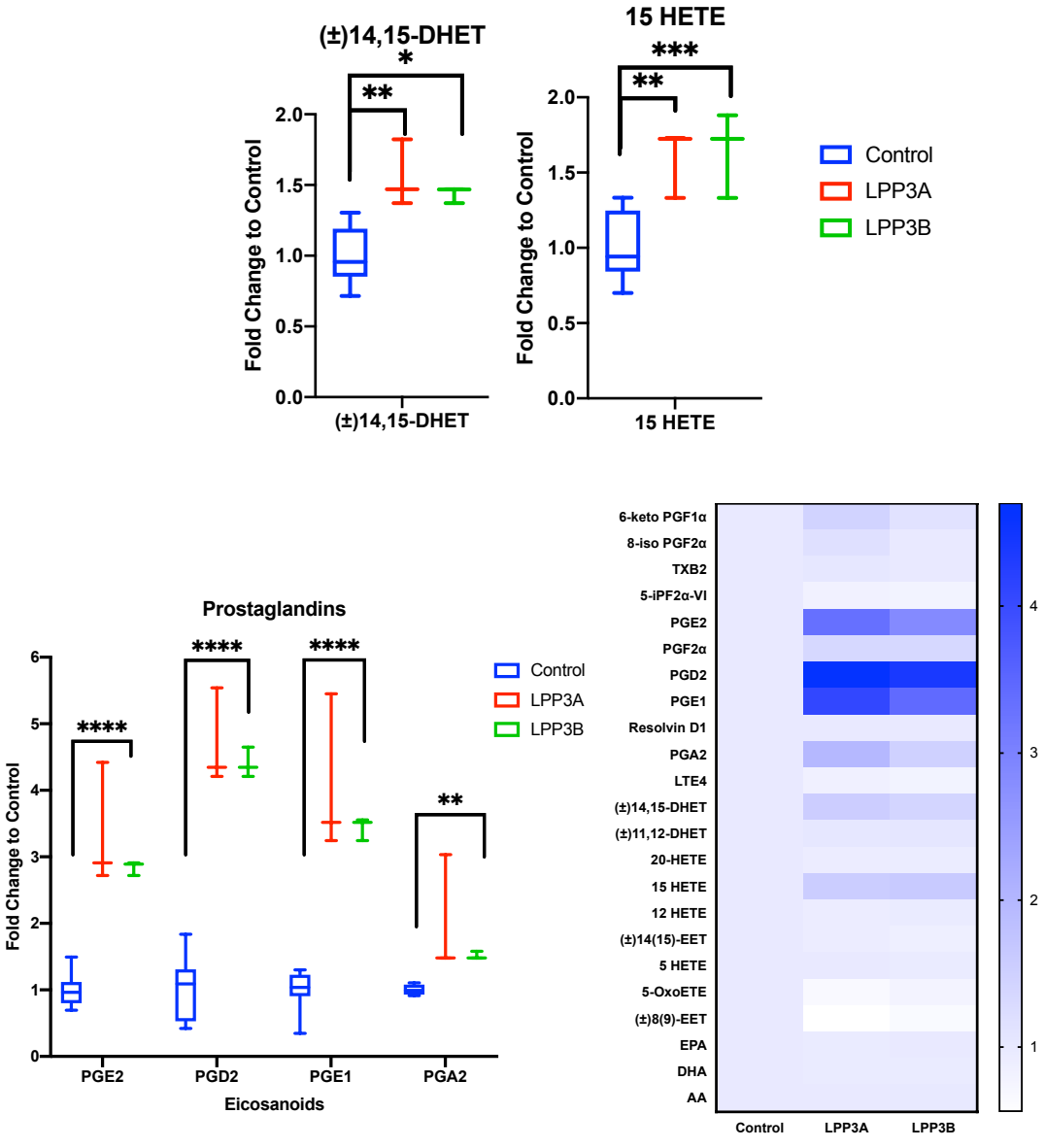

Figure 13 LPP3 eicosanoid analysis
Loss of LPP3 portrays drastic increases in eicosanoid synthesis, due to dysregulation of C1P synthesis.

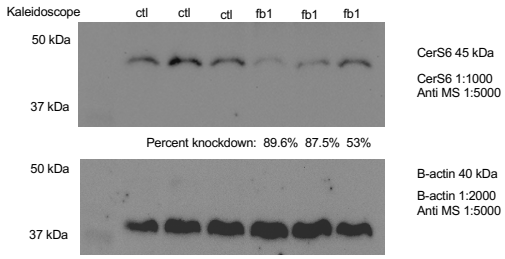

Figure 14 FB1 protein analysis
FB1 treated cells (50 uM for 1 hour) reveals loss of CerS isoforms, protein expression was reduced by over 50%.

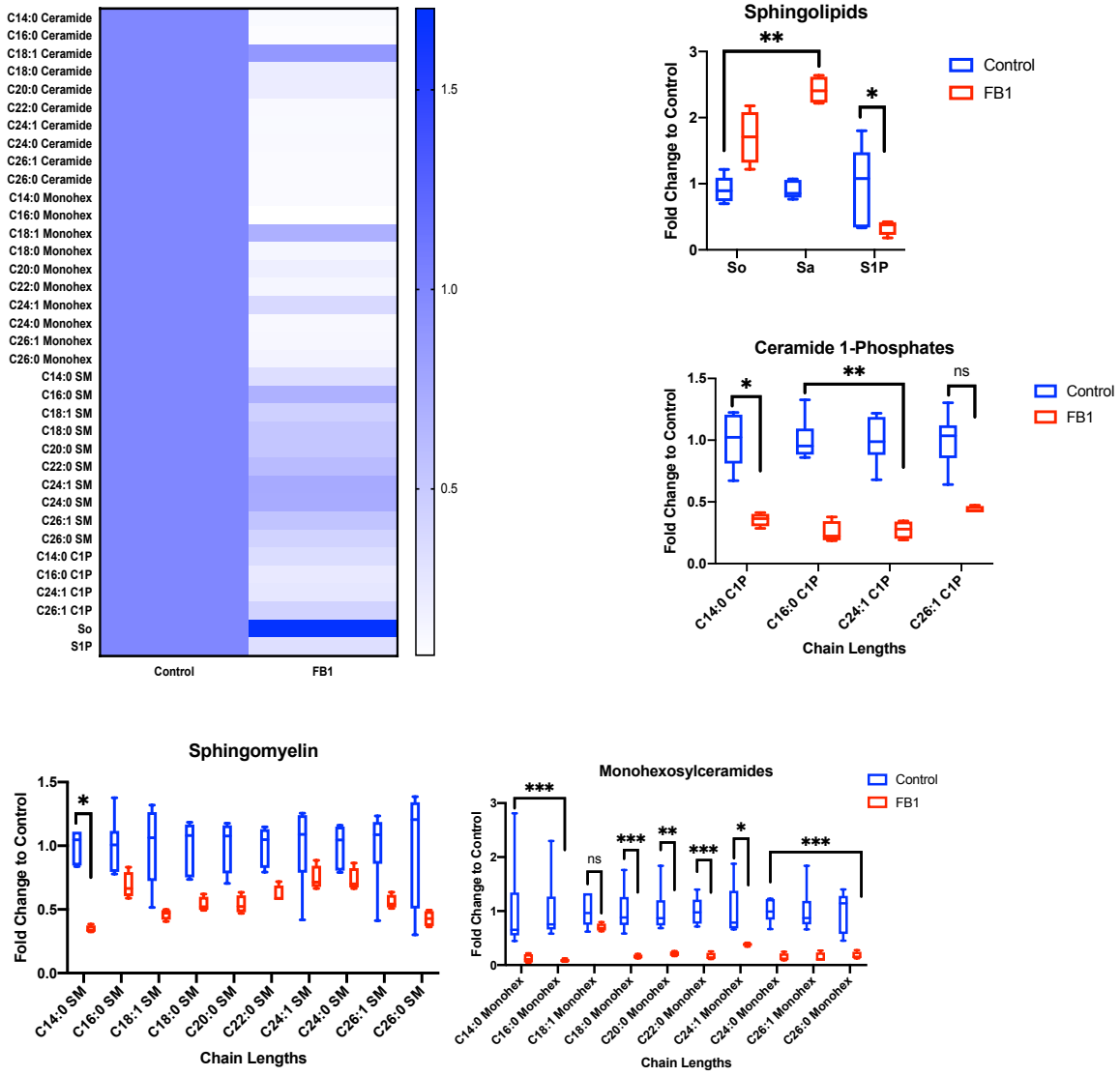

Figure 15 FB1 sphingolipid analysis
When isoforms of CerS are inhibited, accumulation of precursor sphingolipids occurs, resulting in a metabolic imbalance, which is then substantiated in eicosanoid analysis.

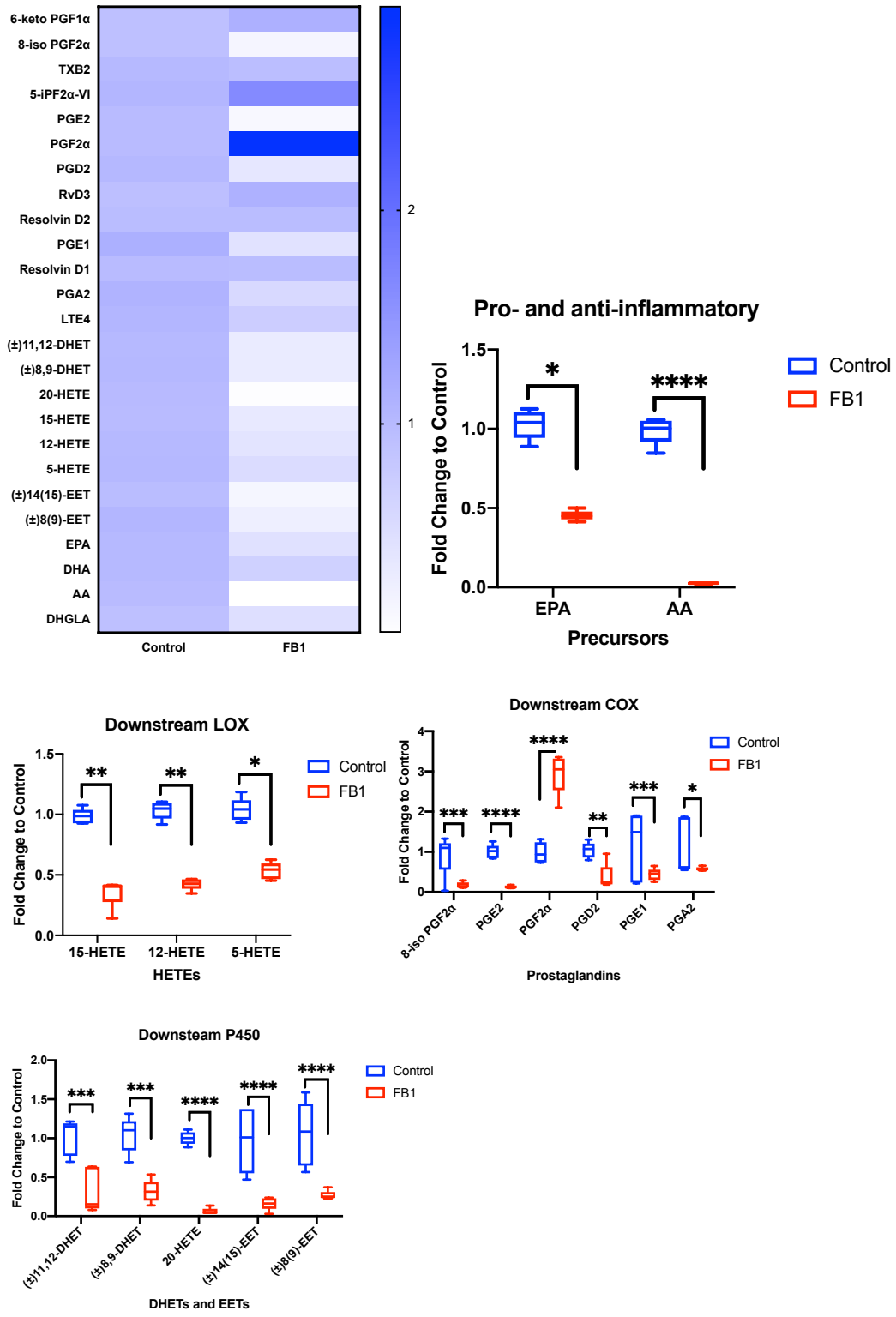

Figure 16 FB1 eicosanoid analysis

In absence of specific isoforms of CerS, anabolism of C1P is inhibited. A compensation phenomenon occurs amongst the other isoforms, as an attempt to make up for the lack of this essential lipid in maintaining cellular balance. Loss of all isoforms of CerS hinders the de novo creation of C1P, thereby perturbing downstream eicosanoids.

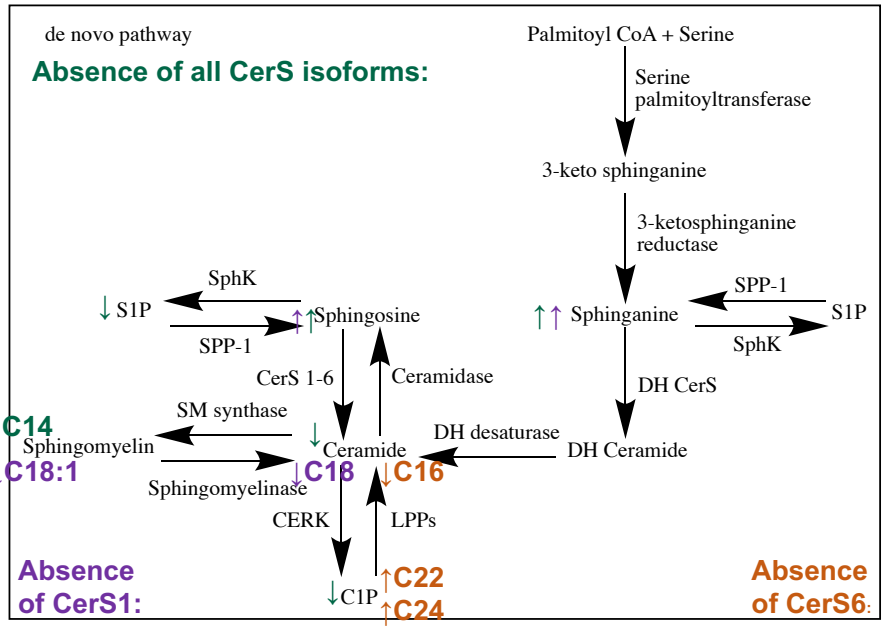

Figure 16 Proposed sphingolipid mechanism

In absence of specific isoforms of CerS, anabolism of C1P is inhibited. A compensation phenomenon occurs amongst the other isoforms, as an attempt to make up for the lack of this essential lipid in maintaining cellular balance. Loss of all isoforms of CerS hinders the de novo creation of C1P, thereby perturbing downstream eicosanoids.

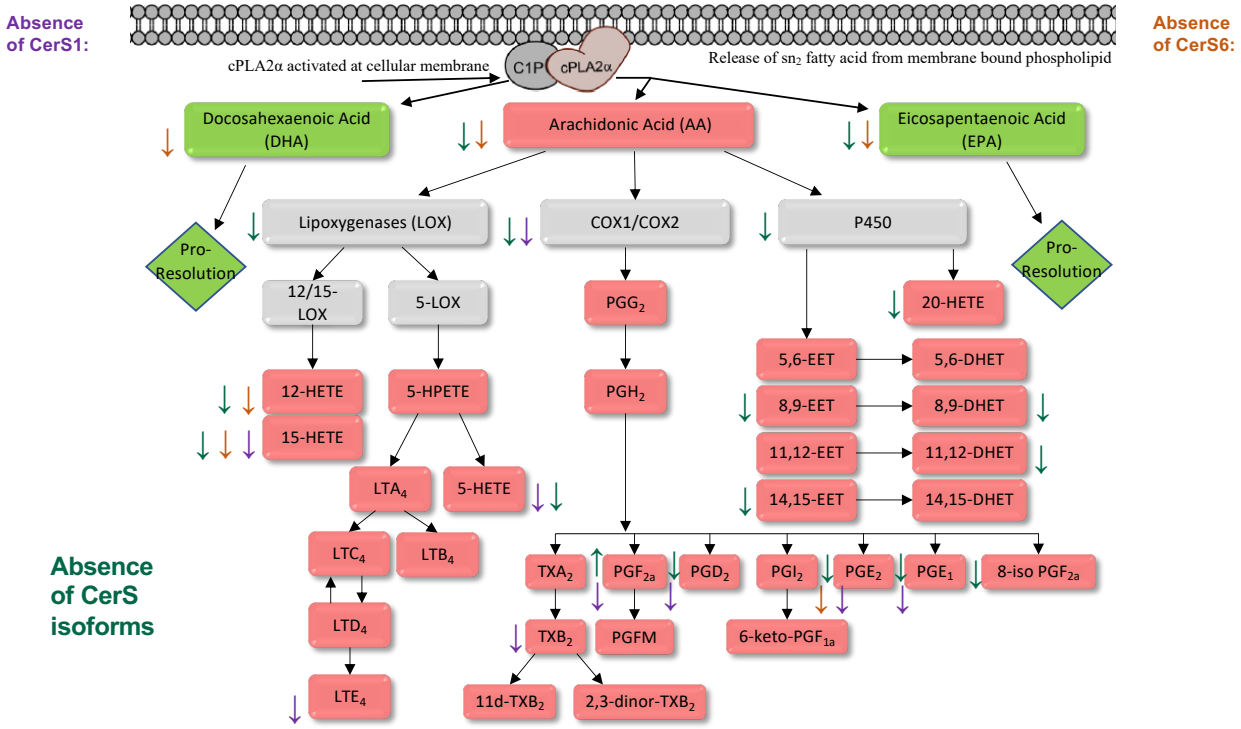

Figure 17 Proposed eicosanoid mechanism
Loss of specific isoforms reveals changes in eicosanoid synthesis, revealing that specific chain lengths of C1P have varying functions in the inflammatory response. Loss of all isoforms using the mycotoxin FB1 portrays similar results to loss of only CerS6, uncovering the important role this isoform plays in creation of C1P

CHAPTER THREE: DETERMINE THE AMOUNT OF C1P FROM THE DE NOVO PATHWAY

Abstract

The dynamic process of wound healing is characterized by four phases: hemostasis, inflammation, proliferation and remodeling[59]. Hemostasis consists of clotting factors, which function to constrict vasculature, thereby decrease bleeding[60]. The wound progresses to the inflammatory phase, which encompasses vasodilation, vascular permeability, and migration of neutrophils and macrophages[61-62]. Once foreign material is expelled, proliferation ensues, wound closure is initiated by fibroblast and keratinocyte migration[63]. Finally, a new epithelial layer is formed, and cross linkage of collagen occurs, resulting in a healed wound with ~80% of original tissue strength[64-65]. Previous work in our lab emphasizes the importance of eicosanoids in wound healing and the role lipids play as potential therapeutics[66]. The interaction between $cPLA_{2\alpha}$ and C1P is essential for eicosanoid synthesis, but how does upstream sphingolipid synthesis effect C1P creation? The goal of this chapter is to **discern if C1P from different pathways have distinct function, and to quantify the amount of C1P which derives from the de novo pathway.** The total amount of C1P which derives from de novo is unknown, as ASM is able to convert SM to Cer for downstream phosphorylation to yield C1P[11]. Further exploration of ASM is required to reveal the total amount of Cer that derives from SM, and whether this pathway of Cer formation is utilized by CERK to yield C1P. NPC1 is similar in function to ASM, both serve to break down precursor lipids and trafficked from

the ER to Golgi[67]. In absence of NPC1, we explore whether this has similar effects as absence of ASM in sphingolipid metabolism, and whether this protein plays a role in C1P metabolism. Delving into the different pathways of C1P generation, whether de novo generated C1P is preferred for $cPLA_{2\alpha}$ interaction and downstream inflammatory processes is unknown. Additionally, examining C1P derived from ASM in comparison to CerS may reveal distinct functions, such as optimal wound healing.

Introduction

ASM is known to create Cer from SM, but it is unknown the amount of C1P which derives from each pathway, respectively. To test this, drug treatments will be used to eliminate respective enzymes from HBEC3-KTs and A549s. Elimination of de novo CerS using FB1 treatment while elimination of ASM will be accomplished by desipramine treatment[68]. Our negative controls for HBEC3-KTs and A549s will be cells treated with the solvent the drug was dissolved in, DMSO. If SM cycle catalyzer ASM is inhibited, then SM specific anabolism of C1P will be absent, then we can determine the total amount of C1P which derives from the de novo pathway **(Fig.5)**. Grouped analysis will be assessed in SPSS to determine the statistical significance between these variables by using a 2-way ANOVA.

NPC1 is a large transmembrane protein found on the membranes of late endosomes, known for cholesterol trafficking **(Fig.19)**. The function of this lysosomal protein is largely uncovered, it is suggested to play a role in transporting multiple substrates by cholesterol regulation[23]. ASM is known to generate Cer from SM **(Fig.5)**, also a required step for cholesterol secretion from late endosomal compartments[22]. To address this, A549s and

HBEC3-KTs will be incubated (300,000 cells per 10 cm dish) transfected with individual siRNA for NPC1 while negative controls will be cells transfected with nontargeting siRNA. Determining the function of NPC in sphingolipid and eicosanoid synthesis will be accomplished utilizing aforementioned extraction process from cell pellets and media with subsequent HPLC/MS analysis. In absence of NPC, we can determine the role it plays in C1P generation by examining sphingolipids and eicosanoids, as well as compare its function to that of ASM.

To determine which pathway generates C1P primarily involved in the inflammatory response, scratch assay will be performed in lung epithelial cells lacking either ASM or CerS. Both cell lines will be incubated (100,000 cells per well on 24-well plate) overnight[69] and treated with respective inhibitors in 2% FBS to serum starve, FB1 (Cayman Chemical, treat 10 uM for 4 hours) for CerS depletion and desipramine treatment (Cayman Chemical, treat 30 uM for 1 hour) for ASM depletion. Using pipette tips to induce mechanical trauma, cells will be monitored for migration in either de novo specific or SM specific synthesis of C1P over a 24-hour time lapse via microscopy (Keyence). Wound healing will be assessed as a migration ratio for each condition, quantified by taking the area immediately following the scratch and the area of the scratch at each respective time point[54]. In order to determine the metabolomic effects of downstream moieties, media for each condition will be saved and extracted for eicosanoid synthesis to determine specific eicosanoids yielded from each pathway.

Materials and Methods

Cancer Cell Lines and Media

The non-small cell lung cancer (NSCLC) cell line A459 and immortalized human bronchial epithelial primary cells (HBEC3-KT) infected with human telomerase (hTERT) and cyclin dependent kinase 4 (CDK4) (purchased from American Type Culture Collection, ATCC) were cultured in DMEM (A549; Gibco) or Airway Epithelial Cell Basal Medium and Bronchial Epithelial Cell Growth Kit (HBEC3-KT; Thermofisher). DMEM was supplemented with 10% fetal bovine serum (FBS, Gibco) and 1% penicillin/streptomycin (Gibco). Cell lines were maintained in an incubator at 37°C with 95% air and 5% CO2. Cells were nourished at 80% confluency. For each cell line, subsequent analysis was performed within the first 10 passages. Prior to harvesting cells for lipid and protein analysis, all samples were rested for 24 hours in DMEM (Gibco) with 2% serum and 1% antibiotic to reduce the adverse effects of serum growth factors on eicosanoid and sphingolipid production.

Protein Extraction and Western Blot Analysis

Cells were harvested on ice in PBS (Gibco), spun down in a microcentrifuge (Sorvall Legend Micro 21R Centrifuge, Thermofisher) at 3.5 RPM for 5 minutes to remove supernatant. Prior to sonication, samples were resuspended in CelLytic lysis regent with 1% protease phosphatase inhibitor (Sigma Aldrich). To decrease viscosity, samples were spun down again. Amount of protein was then quantified using Bradford Protein Assay according to manufacturer's instruction (Bio-Rad).

Samples were prepared for western blot analysis by addition of equal amounts 2x laemmli buffer with 5% beta-mercaptoethanol (Bio-Rad). Samples were then heated at 100 C for 5 minutes, then 15 ug of protein was run on 10% polyacrylamide gels (Bio-Rad) using a PowerPac (Bio-Rad) at 30 mV for 15 minutes and 100 mV for 1.5 hours. Protein was transferred to PVDF membranes using a wet transfer technique according the manufacturer's instructions (Bio-Rad).

Membranes were blocked in 3% nonfat milk in TBST (Bio-Rad) for 1 hour, then blocked overnight at 4 C in primary antibodies outlined in the *Reagents and Antibodies* section. Milk was discarded and membranes were washed in TBST for an hour in 15-minute intervals, then blocked in anti-host secondary antibodies for an additional hour. After discarding milk, a two-hour TBST wash step took place, then membranes were imaged using chemiluminescent HRP substrates (Bio-Rad). Images of protein blots were saved and quantified on Image Lab Software (Bio-Rad), gene silencing was assessed after normalizing protein expression to loading controls.

Drug Treatment

Seeded at 3.0 x 10^5 cells per well in a 6-well plate, lung epithelial cells were grown over a 24 hour period. Drug treatment by 50 uM FB1 (Cayman Chemical) or 70 uM desipramine hydrochloride (Sigma Aldrich) were applied to cells in 2% serum media. Controls included cells treated with solvent drug was resuspended in, DMSO (Dharmacon). After appropriate drug treatment duration, cells were harvested, and media was conserved for successive analysis.

Sphingolipid Extraction

In 6-well plates, lung epithelial cells were harvested in PBS (Gibco), centrifuged and supernatant was removed. Before extraction, samples were temporarily stored at -80 C. Utilizing monophase bligh dry extraction, cell pellets were vortexed in LC/MS grade water optima (Thermofisher). Internal standard was added to each sample vial, vortexed and sonicated to break apart pellets. 2:1 ratio of LC/MS grade methanol to chloroform (Thermofisher) was added, cells were sonicated individually and placed in a 48 C water bath shaker (Precision SWB15, Thermofisher) for 6 hours at 30 RPM. Samples were sonicated prior to centrifugation for 10 min at 4,000 RPM. Organic solvent was transferred to a glass vial and dried down for 2.5 hours (Savant SPD2010 Speedvac Concentrator, Thermofisher). 500uL methanol was added to each sample, sonicated the spun down at 4,000 RPM for 1 minute. Aqueous layer was then transferred to autosampler vials for HPLC-MS analysis

Eicosanoid Extraction

Media from 6-well plates were aliquoted and temporarily saved at -80 C for subsequent analysis using solid phase affinity chromatography. Media was thawed and each sample was prepped for extraction by addition of 100uL methanol, 5uL acetic acid, and 20uL internal standard per mL of media (LC/MS grade, Thermofisher). In a vacuum manifold filter chamber (Agilent Technologies), filter columns were washed by adding 2 mL of methanol, then 2 mL of water (Thermofisher), then sample. To collect misnomer lipids, remaining sample was resuspended in 5% methanol and applied to filter columns. Wash tubes (Falcon) were discarded, and eicosanoids were collected by applied 2 mL

isopropanol (Thermofisher). Samples were then dried down for 5 hours (Savant SPD2010 Speedvac Concentrator, Thermofisher), then redissolved in 50:50 ethanol and water (LC/MS grade, Thermofisher). After vortexing, samples were centrifuged at 5,000 RPM for 15 minutes, then transferred to autosampler vials for HPLC-MS analysis.

HPLC-MS

Using a C18 column (Kinetex), a 14 minute reverse phase LC method was utilized for eicosanoid separation at 50 C with a 200 uL/minute flow rate. Prior to the sample run, column equilibration was accomplished for 10 minutes with 100% Solvent A, a 40:60:0.02 ratio of acetonitrile, water and formic acid (Thermofischer). 10 uL of each sample was injected per run. Within the first minute, 100% Solvent A was used for elution. In a linear gradient, amount of Solvent B- composed of 50:50:0.02 acetonitrile, isopropanol, and formic acid- was increased in a temporal manner by increments of 15%. Towards the end of the run, Solvent B was eluted at 100%. Eicosanoid analytes were quantified by tandem quadrupole mass spectrometer (SciEx Selection). In negative-ion mode, multiple-reaction monitoring of eicosanoids was accomplished using parent ions, which were then fragmented in the collision cell, which yielded product ions of our analytes of interest. These quantitative results were assessed using Quantitation Wizard (Analyst Software, SciEx), then exported for normalization and statistical analysis on Excel (Microsoft Office).

Wound Healing Assay

Lung epithelial cell lines were seeded at confluency of 1.5×10^5 cells per well within 24-well plates. 24 hours later, cells were treated as according to previously stated drug

treatment methods. Mechanical trauma was induced by producing a scratch with a 20uL pipette tip along the diameter of each well[69]. Nonadherent cells were washed with PBS, and placed in an incubation chamber of 5% CO_2 for 24 hour live cell imaging (Keyence VHX-6000). 6 cells from each well were tracked, and migration velocity for each was calculated (VW-9000 software).

Statistical Analysis

Statistically significant data is defined by a p-value equal to or less than 0.05, each value outlined as mean ± standard deviation (SD). Biostatistics analysis utilized either R or GraphPad Prism 8 (GraphPad Prism Software). For comparisons between multiple samples, ANOVA with Tukey post-test were used for subsequent analysis.

Reagent and Antibodies

To assess gene silencing, SMARTpool siRNA for CerS1, CerS6, LPP1 and LPP3 (Dharmacon) was utilized. For specific isoform functional studies, single variants within specific regions need to be targeted utilizing individual siRNA targeting the open reading frame (ORF) for CerS1 (Sigma Aldrich), CerS6 (ON TARGETplus, Dharmacon), LPP1 (FlexiTube Gene Solution, Qiagen) and LPP3 (ON TARGETplus, Dharmacon). Two out of four individual siRNAs within pool were selected for comparison, both achieving a decrease in at least 50% protein expression.

Western blots were performed utilizing the following antibodies: Our loading control was assessed using anti beta-actin antibody (1:2000, Cell Signaling). To validate gene silencing, antibodies for CerS6 (1:1000, Santa Cruz), CerS1 (1:500, abcam), ASM

(1:1000, Invitrogen), and NPC1 (1:100, Novus) were employed. Anti-rabbit and anti-mouse secondary antibodies (1:5000, Cell Signaling) were utilized to reduce appearance of nonspecific proteins.

Results

Effects of de novo C1P generation

ASM is known to create Cer from SM, however, it is unknown the amount of C1P which derives from each respective pathway[49]. In order to determine if CerS or ASM mediated Cer generation is the primary mode of C1P synthesis, eicosanoid analysis will be utilized. By accomplishing decreased expression of ASM **(Fig.20)** and observing changes in eicosanoid synthesis, it can be deduced which pathway plays a larger role in the inflammation and subsequent eicosanoid generation. A decrease in prostaglandin synthesis due to accumulation of AA is observed in ASM absent cells (**Fig.21)**. In absence of CerS isoforms, profound loss in eicosanoids are recorded due lack of AA generation. Some eicosanoids are salvage pathway specific, as an accumulation of PGF2α is observed, portraying this specific prostaglandin is derived from SM synthesis of C1P.

Role of NPC in C1P regulation

NPC1 is largely involved in cholesterol trafficking, but its role in sphingolipid metabolism is unknown. By knock down of this lysosomal protein **(Fig.22)**, we expect a similar phenotype to loss of ASM. This includes accumulation of SM, S1P and precursor sphingolipids, but a lack of Cer and C1P **(Fig.23)**. We expect this will affect downstream eicosanoid synthesis due to unregulated levels of C1P. Lack of NPC1 results in a rare,

genetic, lysosomal storage disease with no cure and a high mortality rate[70]. By unearthing the function of NPC1 in C1P metabolism, it is possible to find targets within sphingolipid biosynthesis for potential targets and therapeutics. Lack of NPC reveals increases in precursor sphingolipids and ceramides, but no increase in C1P production. Eicosanoid production is elevated **(Fig.24)**, similar to lack of LPP3. Because there is no effect on C1P generation, lack of NPC elucidates the relationship between sphingolipid and glycerol synthesis. Without NPC, an accumulation of Cer occurs. SM synthase compensates for this, but rather than increasing SM production, this particular synthase can yield diacylglycerol (DAG) from Cer by donating phosphocholine from phosphotidylcholine (PC) rich membranes[71]. DAG activates PKC, which stimulates an increase in AA production[72], which explains the substantial increase in eicosanoid synthesis when NPC is absent. NPC plays a regulatory role in the synthesis of glycerol and sphingolipid pathways.

Comparison of wound healing rates

By assessing cells lacking either ASM or CerS, we can determine C1P generation derives from de novo or SM pathway specifically. It is unknown the amount of C1P synthesized from each respective pathway. A wound healing assay can help determine the amount from each pathway, as C1P is largely involved in the inflammatory process **(Fig.25)**. We hypothesize de novo generated C1P will portray increased cell migration in the scratch assay, as this is the canonical pathway for C1P, and absence of CerS results in widespread loss of necessary eicosanoids. In absence of enzymes present in each respective pathway, synthesis of specific prostaglandins may be absent or exacerbated

due to compensation. This is essential to expanding the field of lipidomics, as the amount of C1P from de novo has never been quantified, and its effects on wound healing elucidates the importance of these upstream enzymes.

Discussion

In ASM absent cells, it is possible no changes in C1P will be observed, elucidating total C1P is derived exclusively from the de novo pathway. To confirm these effects, mRNA levels may need to be examined by qPCR. When comparing the wound healing rates in absence of ASM or CerS, if there is minimal change between these two pathways, then this elucidates the possibility that C1P primarily derives from the salvage pathway, where S1P is the rate limiting step. To evaluate this, the scratch assay will be performed in cells treated with S1P siRNA to determine how this affects wound healing. However, as S1P is a proposed substrate for CerS, these results may skew C1P derived from the de novo pathway.

Future Directions

The purpose of this research project was to examine the elusive yet detrimental C1P, the means of anabolism and catabolism, as well as how the cell compensates for the loss of upstream enzymatic capabilities. As divulged in this study, de novo synthesis of C1P by CerS6 is crucial to creation of basal inflammatory eicosanoids. To explore the effects on 5-HETE synthesis, studies on activated eicosanoid synthesis by agonist treatment may prove to beneficial for delineating C1P inflammatory synthesis. LPP3 plays

a huge regulatory role in de novo catabolism of C1P, delving into the location of LPP3 is essential for determining where C1P is catabolized within the cell, as well as it's relationship with transporters outside of the golgi. Additionally, by targeting ASM to look into C1P production, it may be possible to rescue these effects by exogenous C1P treatment, in order to circumvent the effects without SM derived C1P.

Conclusions

De novo synthesis of C1P is imperative to eicosanoid production, as shown in this proposed mechanism **(Fig.26)** of C1P synthesis. Eicosanoids are vital to inflammation, wound healing, and cellular migration[48]. Lack of regulation of this multifaceted lipid causes loss of crucial mediators in these processes, as seen in loss of CerS isoforms. Loss of salvage pathway enzyme ASM causes mild effects, including loss of PGF2α. Accumulation of arachidonic acid portrays that salvaged Cer generation yields chain lengths of C1P that are not as essential as de novo creation of C1P. Loss of NPC shows how this moiety may play a regulatory role in the relationship between de novo synthesis and glycerol synthesis, affirmed by accumulation of inflammatory eicosanoids. Exploring the specific pathways in regard to sphingolipid metabolism portrays the importance de novo generation of C16 C1P has on downstream processes.

Figures

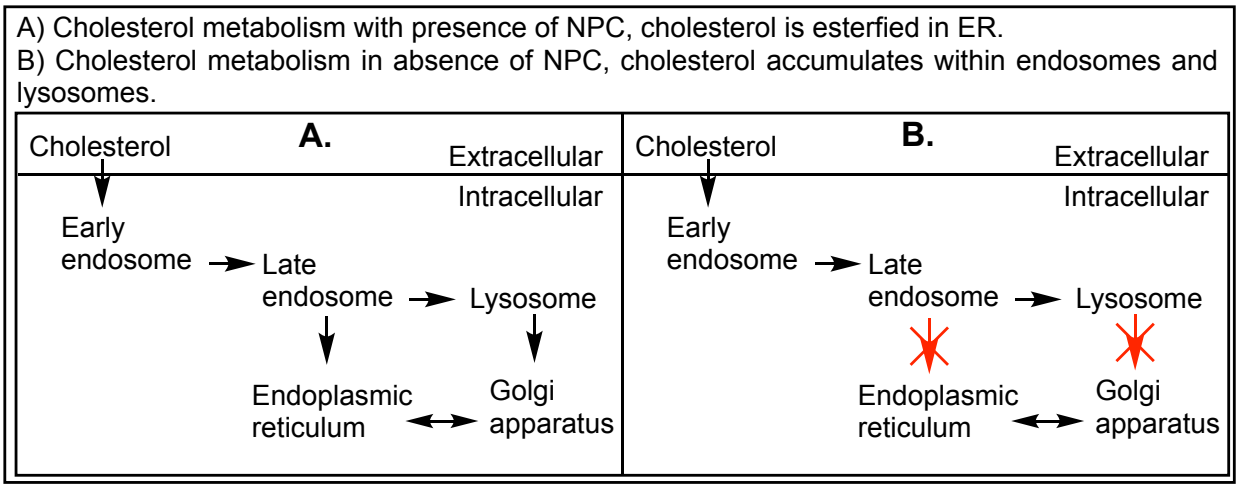

Figure 18 NPC metabolism
Differences in the cell with presence (A) and absence (B) of NPC

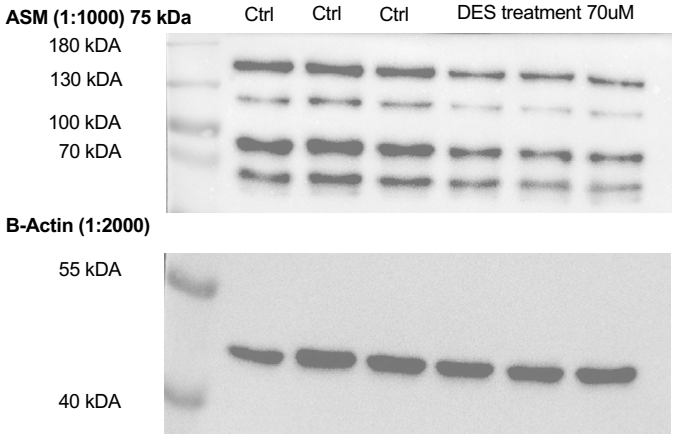

Figure 19 ASM protein analysis
This assay was accomplished in triplicate (n=6), unveiling over 50% decrease in protein expression of ASM, as confirmed by western blot analysis.

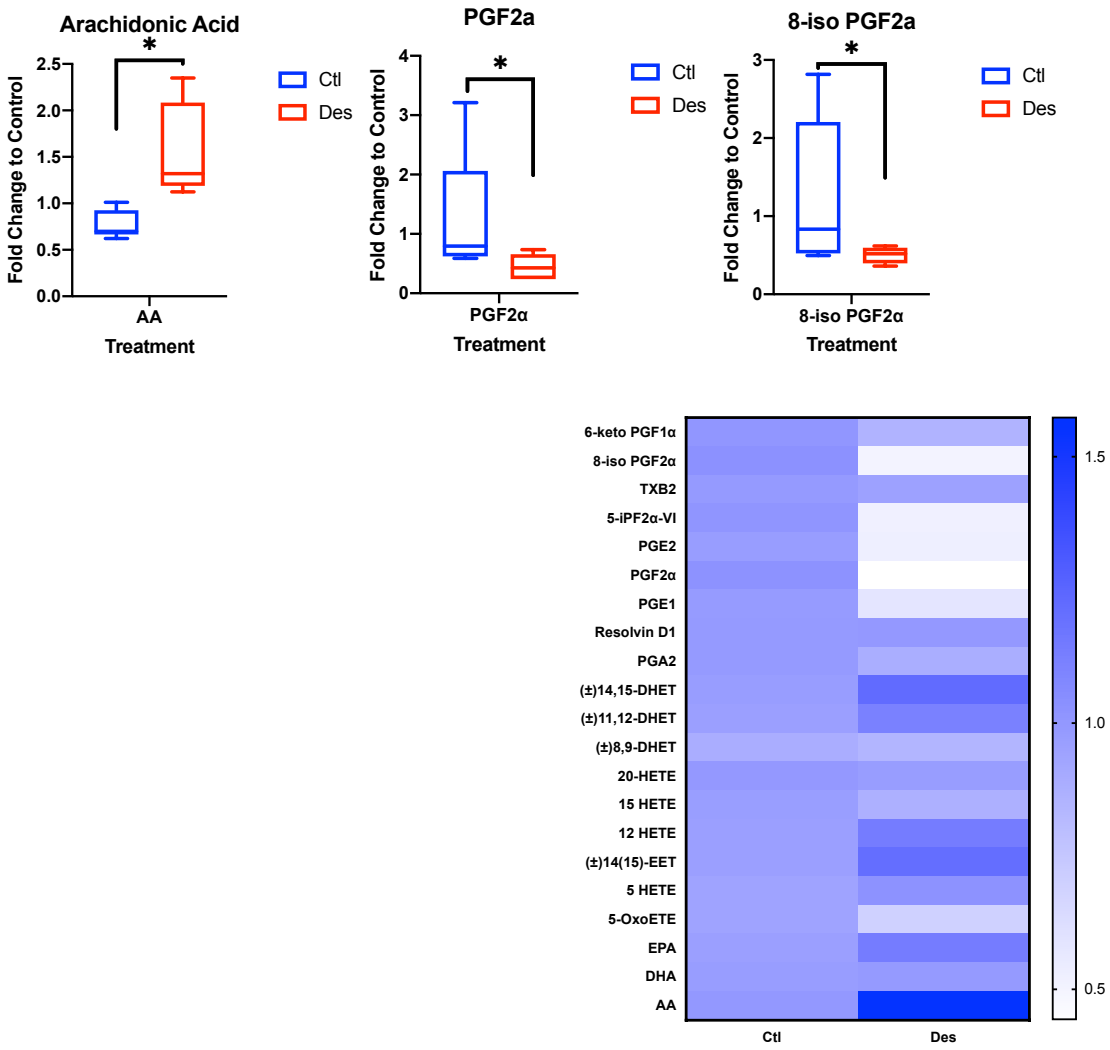

Figure 20 ASM eicosanoid analysis
Analysis of media from cells treated with desipramine. Lack of salvage enzyme ASM inhibits synthesis of prostaglandins due to accumulation of C1P

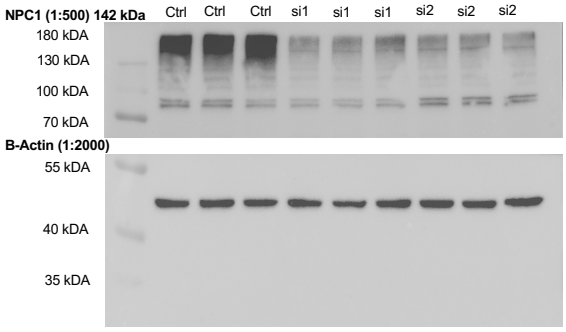

Figure 21 NPC protein analysis
Two different individual siRNAs were used in triplicate (n=6), to verify decreased protein expression of NPC. Protein expression was diminished by over 70% for both silencers.

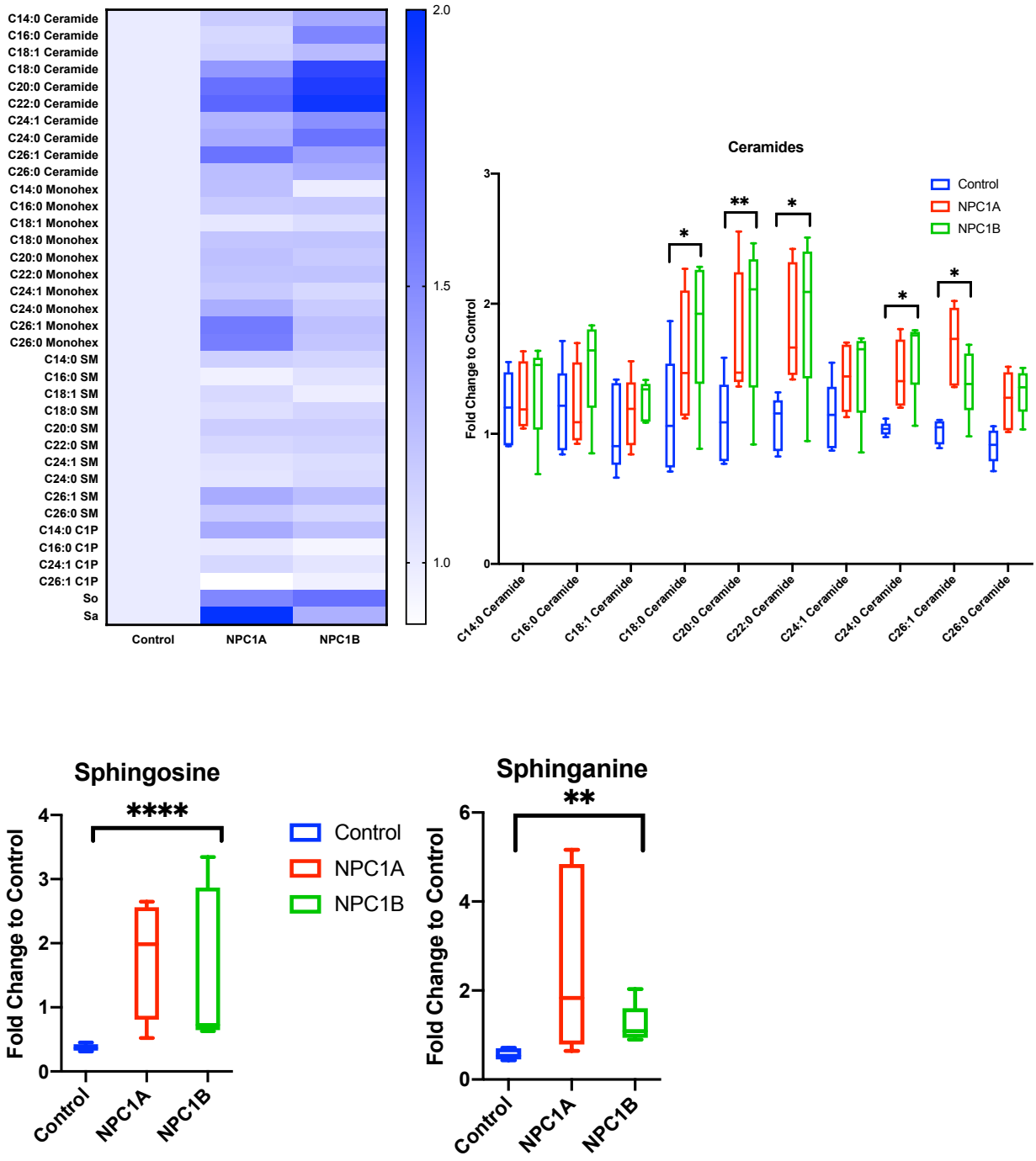

Figure 22 NPC sphingolipid analysis
Absence of NPC reveals accumulation of precursor sphingolipids.

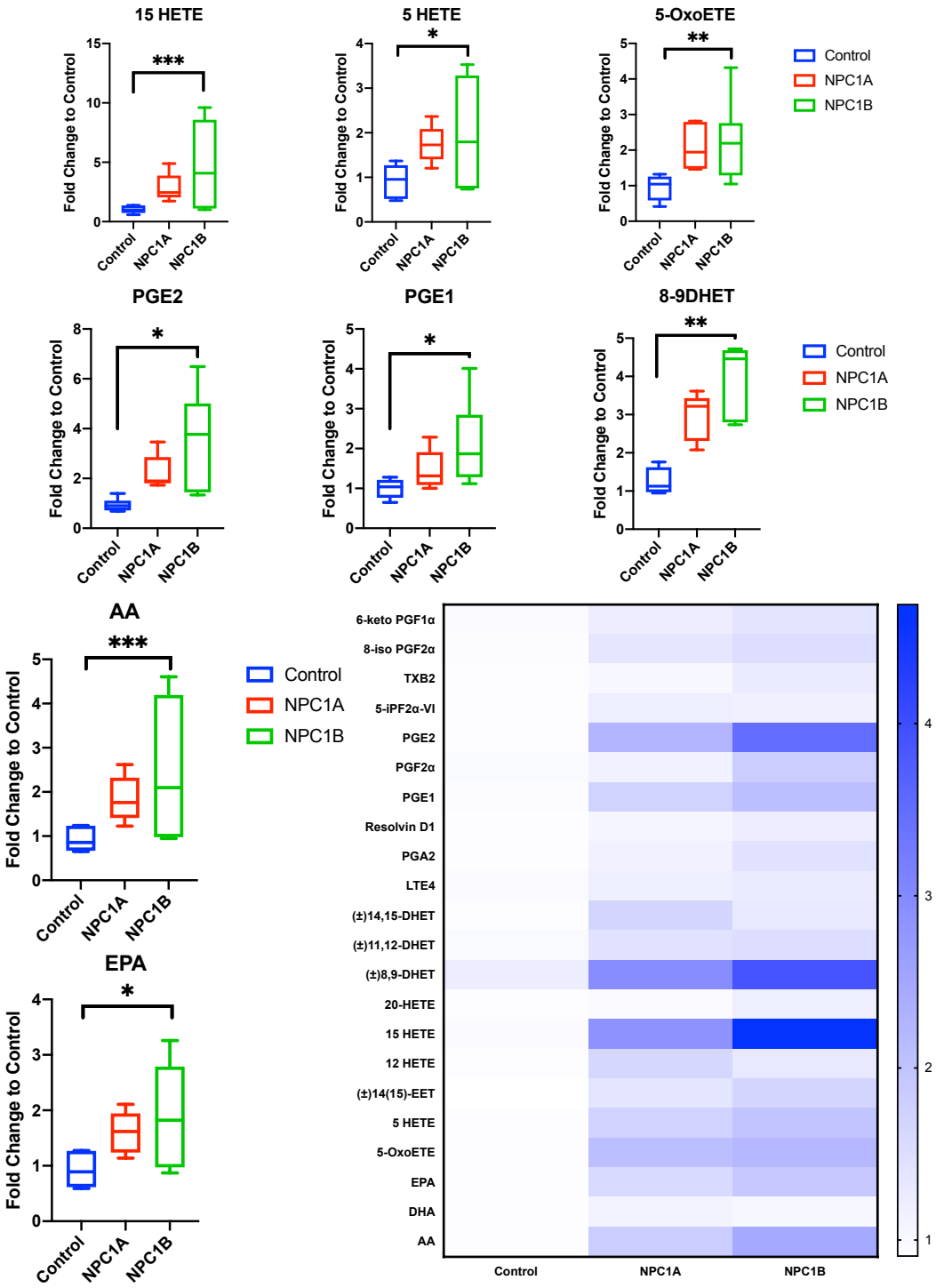

Figure 23 NPC eicosanoid analysis
Lack of NPC results in accumulation of downstream eicosanoids, including pro- and anti-inflammatory mediators

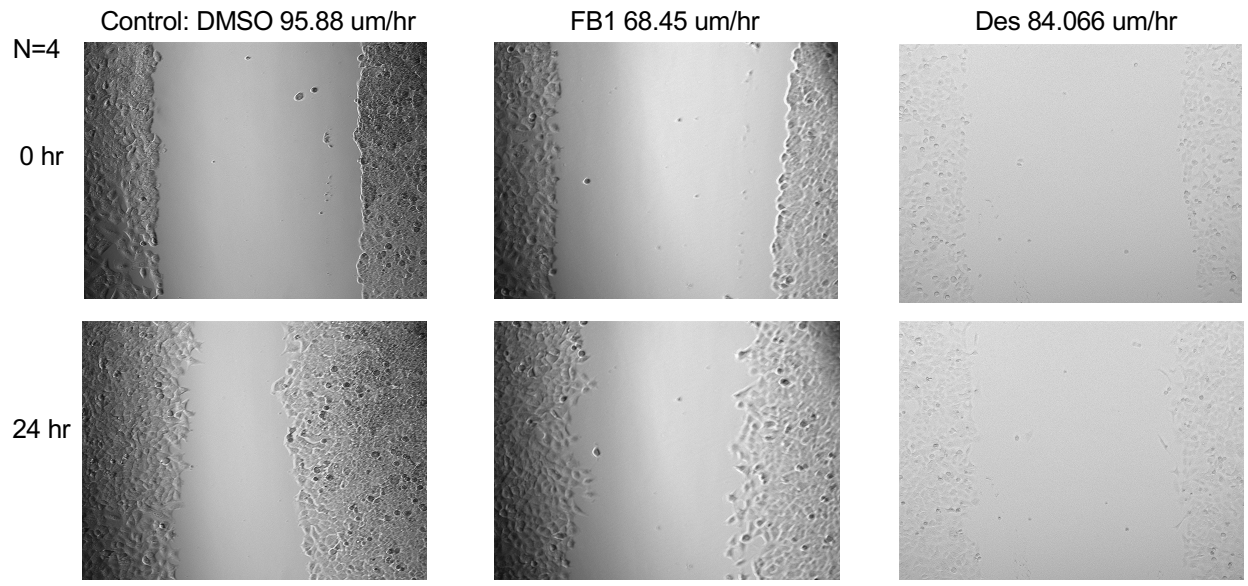

Figure 24 Wound healing assay
Cells exposed to control solvent DMSO, FB1, or DES were tracked for 24 hours to determine effects on cell migration (n=4). Migration velocity averages reveal how treatment hinders the ability of the cell to fill in the scratch on each well.

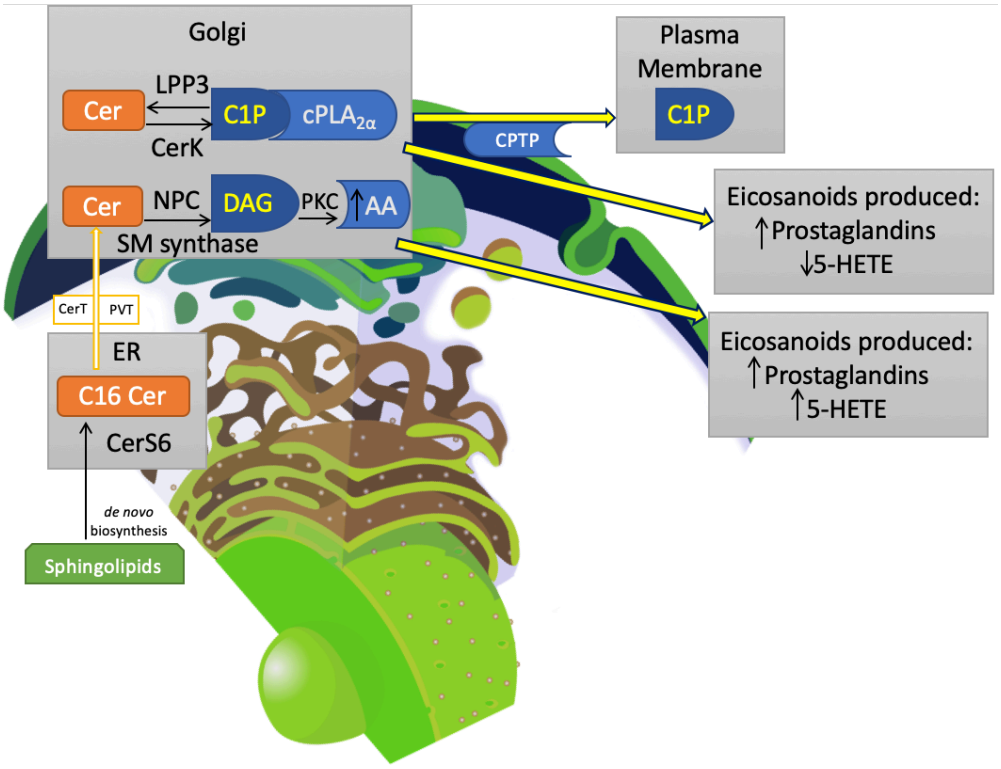

Figure 25 Proposed mechanism
A summary of lipid synthesis and location of metabolites upstream of C1P reveals the importance and regulatory roles of CerS, LPP3, NPC and ASM.

REFERENCES

1. Presa N, Gomez-Larrauri A, Rivera IG, Ordoñez M, Trueba M, Gomez-Muñoz A. Regulation of cell migration and inflammation by ceramide 1-phosphate. Biochim Biophys Acta. 2016 May;1861(5):402-9. **PMID: 26875839**

2. Mitra P, Maceyka M, Payne SG, Lamour N, Milstien S, Chalfant CE, Spiegel S. Ceramide kinase regulates growth and survival of A549 human lung adenocarcinoma cells. FEBS Lett. 2007 Feb 20;581(4):735-40. **PMID: 17274985**

3. D.J. Stephenson, L.A. Hoeferlin, C.E. Chalfant Lipidomics in translational research and the clinical significance of lipid-based biomarkers Transl. Res., 189 (2017), pp. 13-29. **PMID: 28668521**

4. Wijesinghe DS, Massiello A, Subramanian P, Szulc Z, Bielawska A, Chalfant CE. Substrate specificity of human ceramide kinase. J Lipid Res. 2005 Dec;46(12):2706-16 **PMID: 16170208**

5. Xu Z, Zhou J, McCoy DM, Mallampalli RK. LASS5 is the predominant ceramide synthase isoform involved in de novo sphingolipid synthesis in lung epithelia. J Lipid Res. 2005; 46:1229–1238. **PMID: 15772421**

6. Kai M, Wada I, Imai Si, Sakane F, Kanoh H. Cloning and characterization of two human isozymes of Mg2+-independent phosphatidic acid phosphatase. J Biol Chem. 1997 Sep 26;272(39):24572-8. **PMID: 9305923**

7. Leiber D, Banno Y, Tanfin Z. Exogenous sphingosine 1-phosphate and sphingosine kinase activated by endothelin-1 induced myometrial contraction through differential mechanisms. Am J Physiol Cell Physiol. 2007 Jan; **PMID: 16956968**

8. Newton J, Milstien S, Spiegel S. Niemann-Pick type C disease: The atypical sphingolipidosis. Adv Biol Regul. 2018 Dec;70:82-88. doi: 10.1016/j.jbior.2018.08.001. Epub 2018 Aug 28. **PMID: 30205942**

9. A.H. Merrill Jr., E.M. Schmelz, D.L. Dillehay, S. Spiegel, J.A. Shayman, E. Wang Sphingolipids--the enigmatic lipid class: Biochemistry, physiology, and pathophysiology Toxicology and Applied Pharmacology, 142 (1) (1997), pp. 208-225. **PMID: 9007051**

10. Nadia F. Lamour, Preeti Subramanian, Dayanjan S. Wijesinghe, Robert V. Stahelin, Joseph V. Bonventre, Charles E. Chalfant. Ceramide 1-Phosphate Is Required for the Translocation of Group IVA Cytosolic Phospholipase A_2 and Prostaglandin Synthesis. Journal of Biol. Chem. (2009) 284: 26897-. doi:10.1074/jbc.M109.001677. **PMID: 19632995**

11. Charles E. Chalfant, Sarah Spiegel Sphingosine 1-phosphate and ceramide 1-phosphate: expanding roles in cell signaling. Journal of Cell Science. 2005. 118: 4605-4612; doi: 10.1242/jcs.02637. **PMID: 16219683**

12. Sridevi P, Alexander H, Laviad EL, Min J, Mesika A, Hannink M, Futerman AH, Alexander S. Stress-induced ER to Golgi translocation of ceramide synthase 1 is dependent on proteasomal processing. Exp Cell Res. 2010 Jan 1;316(1):78-91. doi: 10.1016/j.yexcr.2009.09.027. **PMID: 19800881**

13. Venkataraman K, Riebeling C, Bodennec J, Riezman H, Allegood JC, Sullards MC, Merrill AH, Jr, Futerman AH. Upstream of growth and differentiation factor 1 (uog1), a mammalian homolog of the yeast longevity assurance gene 1 (LAG1), regulates N-stearoyl-sphinganine (C18-(dihydro)ceramide) synthesis in a fumonisin B1-independent manner in mammalian cells. J Biol Chem. 2002;277:35642–9. **PMID: 12105227**

14. Senkal CE, Ponnusamy S, Rossi MJ, Bialewski J, Sinha D, Jiang JC, Jazwinski SM, Hannun YA, Ogretmen B. Role of human longevity assurance gene 1 and C18-ceramide in chemotherapy-induced cell death in human head and neck squamous cell carcinomas. Mol Cancer Ther. 2007;6:712–22. **PMID: 17308067**

15. Levy M, Futerman AH. Mammalian ceramide synthases. IUBMB Life. 2010 May;62(5):347-56. doi: 10.1002/iub.319. **PMID: 20222015**

16. Becker I, Wang-Eckhardt L, Yaghootfam A, Gieselmann V, Eckhardt M. Differential expression of (dihydro)ceramide synthases in mouse brain: oligodendrocyte-specific expression of CerS2/Lass2. Histochem Cell Biol. 2008;129:233–241 **PMID: 17901973**

17. Gehring WJ, Affolter M, Burglin T. Homeodomain proteins. Annu Rev Biochem. 1994;63:487–526. **PMID: 7979246**

18. Mesika A, Ben-Dor S, Laviad EL, Futerman AH. A new functional motif in Hox domain-containing ceramide synthases: identification of a novel region flanking the Hox and TLC domains essential for activity. J Biol Chem. 2007;282:27366–27373. **PMID: 17609214**

19. Enric Gutiérrez-Martínez, Inés Fernández-Ulibarri, Francisco Lázaro-Diéguez, Ludger Johannes, Susan Pyne, Elisabet Sarri, Gustavo Egea. Lipid phosphate phosphatase 3 participates in transport carrier formation and protein trafficking in the early secretory pathway. Journal of Cell Science. (2013) 126: 2641-2655; doi: 10.1242/jcs.117705. **PMID: 23591818**

20. Pyne S, Kong KC, Darroch PI. Lysophosphatidic acid and sphingosine 1-phosphate biology: the role of lipid phosphate phosphatases. Semin Cell Dev Biol. 2004 Oct;15(5):491-501. doi: 10.1016/j.semcdb.2004.05.007. PMID: 15271294.

21. Jean-Pierre Jaffrézou, Nicolas Maestre, Veronique De Mas-mansat, Christine Bezombes, Thierry Levade, Guy Laurent. Positive feedback control of neutral sphingomyelinase activity by ceramide. The FASEB Journal. (1998) 12:11, 999-1006. **PMID: 9707172**

22. Justice MJ, Bronova I, Schweitzer KS, Poirier C, Blum JS, Berdyshev EV, Petrache I. Inhibition of acid sphingomyelinase disrupts LYNUS signaling and triggers autophagy. J Lipid Res. 2018 Apr;59(4):596-606. doi: 10.1194/jlr.M080242. Epub 2018 Jan 29. **PMID: 29378782**

23. Bräuer AU, Kuhla A, Holzmann C, Wree A, Witt M. Current Challenges in Understanding the Cellular and Molecular Mechanisms in Niemann-Pick Disease Type C1. Int J Mol Sci. 2019 Sep 6;20(18):4392. doi: 10.3390/ijms20184392. **PMID: 31500175**

24. Gomez-Munoz A, Kong JY, Salh B, Steinbrecher UP. Ceramide-1-phosphate blocks apoptosis through inhibition of acid sphingomyelinase in macrophages. J Lipid Res. 2004;45(1):99–105 **PMID: 14523050**

25. Tang X, Benesch MG, Brindley DN. Lipid phosphate phosphatases and their roles in mammalian physiology and pathology. J Lipid Res. 2015 Nov;56(11):2048-60. doi: 10.1194/jlr.R058362. Epub 2015 Mar 26. **PMID: 25814022**

26. Höglinger D, Burgoyne T, Sanchez-Heras E, Hartwig P, Colaco A, Newton J, Futter CE, Spiegel S, Platt FM, Eden ER. NPC1 regulates ER contacts with endocytic organelles to mediate cholesterol egress. Nat Commun. 2019 Sep 19;10(1):4276. doi: 10.1038/s41467-019-12152-2. **PMID: 31537798**

27. Pacheco CD, Lieberman AP. The pathogenesis of Niemann-Pick type C disease: a role for autophagy? Expert Rev Mol Med. 2008 Sep 10;10:e26. doi: 10.1017/S146239940800080X. **PMID: 18782459**

28. Buchman TG, Simpson SQ, Sciarretta KL, Finne KP, Sowers N, Collier M, Chavan S, Oke I, Pennini ME, Santhosh A, Wax M, Woodbury R, Chu S, Merkeley TG, Disbrow GL, Bright RA, MaCurdy TE, Kelman JA. Sepsis Among Medicare Beneficiaries: 1. The Burdens of Sepsis, 2012-2018. Crit Care Med. 2020 Mar;48(3):276-288. doi: 10.1097/CCM.0000000000004224. **PMID: 32058366**

29. Nadia F. Lamour, Preeti Subramanian, Dayanjan S. Wijesinghe, Robert V. Stahelin, Joseph V. Bonventre, Charles E. Chalfant. Ceramide 1-Phosphate Is Required for the Translocation of Group IVA Cytosolic Phospholipase A_2 and Prostaglandin Synthesis. Journal of Biol. Chem. (2009) 284: 26897-. doi:10.1074/jbc.M109.001677. **PMID: 19632995**

30. Pettus B. J., Bielawska A., Spiegel S., Roddy P., Hannun Y. A., Chalfant C. E. 2003. Ceramide kinase mediates cytokine and calcium ionophore-induced arachidonic acid release. J. Biol. Chem. 2783: 38206–38213. **PMID: 12855693**

31. Murakami M, Nakatani Y, Kudo I. 1996. Type II secretory phospholipase A2 associated with cell surfaces via C-terminal heparin-binding lysine residues augments stimulus-initiated delayed prostaglandin generation. J Biol Chem. **PMID: 8939951**

32. Dai SX, Li WX, Li GH, Huang JF. Proteome-wide prediction of targets for aspirin: new insight into the molecular mechanism of aspirin. PeerJ. 2016 Mar 10;4:e1791. doi: 10.7717/peerj.1791. **PMID: 26989626**

33. Singh RK, Ethayathulla AS, Jabeen T, Sharma S, Kaur P, Singh TP. 2005. Aspirin induces its anti-inflammatory effects through its specific binding to phospholipase A(2): crystal structure of the complex formed between phospholipase A(2) and aspirin at 1.9 angstrom resolution. Journal of Drug Targeting. 2005;13:113–119. **PMID: 15823962**

34. Rudd KE, Johnson SC, Agesa KM, Shackelford KA, Tsoi D, Kievlan DR, Colombara DV, Ikuta KS, Kissoon N, Finfer S, Fleischmann-Struzek C, Machado FR, Reinhart KK, Rowan K, Seymour CW, Watson RS, West TE, Marinho F, Hay SI, Lozano R, Lopez AD, Angus DC, Murray CJL, Naghavi M. Global, regional, and national sepsis incidence and mortality, 1990-2017: analysis for the Global Burden of Disease Study. Lancet. 2020 Jan 18;395(10219):200-211. **PMID: 31954465**

35. Rello J, Valenzuela-Sánchez F, Ruiz-Rodriguez M, Moyano S. Sepsis: A Review of Advances in Management. Adv Ther. 2017. Nov;34(11):2393-2411. doi: 10.1007/s12325-017-0622-8. **PMID: 29022217**

36. Martin GS. Sepsis, severe sepsis and septic shock: Changes in incidence, pathogens and outcomes. Expert Rev Anti Infect Ther 2012; 10:701–706. **PMID: 22734959**

37. Hiemstra PS, McCray PB Jr, Bals R. The innate immune function of airway epithelial cells in inflammatory lung disease. Eur Respir J. 2015 Apr;45(4):1150-62. PMID: 25700381

38. Gault CR, Obeid LM, Hannun YA. An overview of sphingolipid metabolism: from synthesis to breakdown. Adv Exp Med Biol. 2010;688:1-23. doi: 10.1007/978-1-4419-6741-1_1. PMID: 20919643

39. Enric Gutiérrez-Martínez, Inés Fernández-Ulibarri, Francisco Lázaro-Diéguez, Ludger Johannes, Susan Pyne, Elisabet Sarri, Gustavo Egea. Lipid phosphate phosphatase 3 participates in transport carrier formation and protein trafficking in the early secretory pathway. Journal of Cell Science. (2013) 126: 2641-2655; doi: 10.1242/jcs.117705. **PMID: 23591818**

40. Liu N, Li Y, Su S, Wang N, Wang H, Li J. Inhibition of cell migration by ouabain in the A549 human lung cancer cell line. Oncol Lett. 2013 Aug;6(2):475-479. doi: 10.3892/ol.2013.1406. Epub 2013 Jun 17. PMID: 24137350

41. Wang, E., W. P. Norred, C. W. Bacon, R. T. Riley, and A. H. Merrill, Jr. 1991. Inhibition of sphingolipid biosynthesis by fumonisins. Implications for diseases

associated with Fusarium moniliforme. J Biol Chem 266: 14486-14490. PMID: 1860857

42. Merrill AH Jr, Sullards MC, Wang E, Voss KA, Riley RT. Sphingolipid metabolism: roles in signal transduction and disruption by fumonisins. Environ Health Perspect. 2001 May;109 Suppl 2(Suppl 2):283-9. doi: 10.1289/ehp.01109s2283. PMID: 11359697

43. Hu W, Huang J, Mahavadi S, Li F, Murthy KS. Lentiviral siRNA silencing of sphingosine-1-phosphate receptors S1P1 and S1P2 in smooth muscle. Biochem Biophys Res Commun. 2006 May 19;343(4):1038-44. PMID: 16574065

44. Jose L.Tomsig, Ashley H.Snyder, Evgeny V.Berdyshev,Anastasia Skobeleva, Chifundo Mataya, Viswanathan Natarajan, David N. Brindle, Kevin R. Lynch. Lipid phosphate phosphohydrolase type 1 (LPP1) degrades extracellular lysophosphatidic acid *in vivo* Biochem J. 2009 May 1; 419(3): 611–618. PMID: 19215222

45. Bionda C, Portoukalian J, Schmitt D, Rodriguez-Lafrasse C, Ardail D. Subcellular compartmentalization of ceramide metabolism: MAM (mitochondria-associated membrane) and/or mitochondria? Biochem J. 2004 Sep 1;382(Pt 2):527-33. doi: 10.1042/BJ20031819. PMID: 15144238;

46. Le Stunff H, Galve-Roperh I, Peterson C, Milstien S, Spiegel S. Sphingosine-1-phosphate phosphohydrolase in regulation of sphingolipid metabolism and apoptosis. J Cell Biol. 2002 Sep 16;158(6):1039-49. doi: 10.1083/jcb.200203123. Epub 2002 Sep 16. PMID: 12235122

47. Bligh EG, Dyer WJ. A rapid method of total lipid extraction and purification. Canadian Journal of. Canadian Journal of Biochemistry and Physiology. 1959;37(8):911–917. PMID: 13671378

48. Simanshu DK, Kamlekar R-K, Wijesinghe DS, Zou X, Zhai X, Mishra SK, Molotkovsky JG, Malinina L, Hinchcliffe EH, Chalfant CE, Brown RE, Patel DJ. Non-vesicular trafficking by a ceramide-1-phosphate transfer protein regulates eicosanoids. Nature. 2013;500:463–467 PMID: 23863933

49. Berwick M.L., Dudley B.A., Maus K., Chalfant C.E. (2019) The Role of Ceramide 1-Phosphate in Inflammation, Cellular Proliferation, and Wound Healing. In: Stiban J. (eds) Bioactive Ceramides in Health and Disease. Advances in Experimental Medicine and Biology, vol 1159. Springer, Cham. PMID: 31502200

50. Leiber D, Banno Y, Tanfin Z. Exogenous sphingosine 1-phosphate and sphingosine kinase activated by endothelin-1 induced myometrial contraction through differential mechanisms. Am J Physiol Cell Physiol. 2007 Jan; PMID: 16956968

51. Jiang Z, Zhang H. Molecular Mechanism of S1P Binding and Activation of the $S1P_1$ Receptor. J Chem Inf Model. 2019 Oct 28;59(10):4402-4412. doi: 10.1021/acs.jcim.9b00642. Epub 2019 Oct 15. PMID: 31589433.

52. Zelnik ID, Rozman B, Rosenfeld-Gur E, Ben-Dor S, Futerman AH. A Stroll Down the CerS Lane. Adv Exp Med Biol. 2019;1159:49-63. doi: 10.1007/978-3-030-21162-2_4. PMID: 31502199.

53. Wang T, Fu X, Chen Q, Patra JK, Wang D, Wang Z, Gai Z. Arachidonic Acid Metabolism and Kidney Inflammation. Int J Mol Sci. 2019 Jul 27;20(15):3683. doi: 10.3390/ijms20153683. PMID: 31357612; PMCID: PMC6695795.

54. Jasinska R, Zhang QX, Pilquil C, Singh I, Xu J, Dewald J, Dillon DA, Berthiaume LG, Carman GM, Waggoner DW, Brindley DN. Lipid phosphate phosphohydrolase-1 degrades exogenous glycerolipid and sphingolipid phosphate esters. Biochem J. 1999 Jun 15;340 (Pt 3)(Pt 3):677-86. PMID: 10359651; PMCID: PMC1220298.

55. Fettel J, Kühn B, Guillen NA, Sürün D, Peters M, Bauer R, Angioni C, Geisslinger G, Schnütgen F, Meyer Zu Heringdorf D, Werz O, Meybohm P, Zacharowski K, Steinhilber D, Roos J, Maier TJ. Sphingosine-1-phosphate (S1P) induces potent anti-inflammatory effects in vitro and in vivo by S1P receptor 4-mediated suppression of 5-lipoxygenase activity. FASEB J. 2019 Feb;33(2):1711-1726. doi: 10.1096/fj.201800221R. Epub 2018 Sep 6. PMID: 30188757.

56. Hait NC, Maiti A. The Role of Sphingosine-1-Phosphate and Ceramide-1-Phosphate in Inflammation and Cancer. Mediators Inflamm. 2017;2017:4806541. doi: 10.1155/2017/4806541. Epub 2017 Nov 15. PMID: 29269995; PMCID: PMC5705877.

57. Plöhn S, Edelmann B, Japtok L, He X, Hose M, Hansen W, Schuchman EH, Eckstein A, Berchner-Pfannschmidt U. CD40 Enhances Sphingolipids in Orbital Fibroblasts: Potential Role of Sphingosine-1-Phosphate in Inflammatory T-Cell Migration in Graves' Orbitopathy. Invest Ophthalmol Vis Sci. 2018 Nov 1;59(13):5391-5397. doi: 10.1167/iovs.18-25466. PMID: 30452592.

58. Savić R, Schuchman EH. Use of acid sphingomyelinase for cancer therapy. Adv Cancer Res. 2013;117:91-115. doi: 10.1016/B978-0-12-394274-6.00004-2. PMID: 23290778.

59. Marino GK, Santhiago MR, Torricelli AA, Santhanam A, Wilson SE. Corneal Molecular and Cellular Biology for the Refractive Surgeon: The Critical Role of the

Epithelial Basement Membrane. J Refract Surg. 2016 Feb;32(2):118-25. PMID: 26856429

60. Versteeg HH, Heemskerk JWM, Levi M, Reitsma PH. New Fundamentals in Hemostasis. 2013. Physiol Rev. PMID: 23303912
61. Kim M-H, Liu W, Borjesson DL, Curry F-RE, Miller LS, Cheung AL. Dynamics of neutrophil infiltration during cutaneous wound healing and infection using fluorescence imaging. J Invest Dermatol 2008 Jul;128(7):1812–20 PMID: 18185533
62. Eming SA, Wynn TA, Martin P. Inflammation and metabolism in tissue repair and regeneration. Science. 2017 Jun 9. 356(6342):1026–30. PMID: 28596335
63. Sivamani RK. Eicosanoids and Keratinocytes in Wound Healing. Adv wound care. 2014 Jul 1;3(7):476–81. PMID: 25032067
64. Rodrigues M, Kosaric N, Bonham CA, Gurtner GC. Wound Healing: A Cellular Perspective. Physiol Rev. 2019. 99(1):665–706. PMID: 30475656
65. Morris JL, Cross SJ, Lu Y, Kadler KE, Lu Y, Dallas SL. Live imaging of collagen deposition during skin development and repair in a collagen I – GFP fusion transgenic zebrafish line. Dev Biol. 2018. PMID: 29883658
66. MacKnight HP, Stephenson DJ, Hoeferlin LA, Benusa SD, DeLigio JT, Maus KD, Ali AN, Wayne JS, Park MA, Hinchcliffe EH, Brown RE, Ryan JJ, Diegelmann RF, Chalfant CE. The interaction of ceramide 1-phosphate with group IVA cytosolic phospholipase A2 coordinates acute wound healing and repair. Sci Signal. 2019 Dec 3;12(610). PMID: 31796632

67. Liu N, Li Y, Su S, Wang N, Wang H, Li J. Inhibition of cell migration by ouabain in the A549 human lung cancer cell line. Oncol Lett. 2013 Aug;6(2):475-479. doi: 10.3892/ol.2013.1406. Epub 2013 Jun 17. PMID: 24137350

68. Cockburn CL, Green RS, Damle SR, Martin RK, Ghahrai NN, Colonne PM, Fullerton MS, Conrad DH, Chalfant CE, Voth DE, Rucks EA, Gilk SD, Carlyon JA. Functional inhibition of acid sphingomyelinase disrupts infection by intracellular bacterial pathogens. Life Sci Alliance. 2019 Mar 22;2(2):e201800292. doi: 10.26508/lsa.201800292. PMID: 30902833

69. Martinotti S., Ranzato E. (2019) Scratch Wound Healing Assay. In: Turksen K. (eds) Epidermal Cells. Methods in Molecular Biology, vol 2109. Humana, New York, NY

70. Geberhiwot T, Moro A, Dardis A, Ramaswami U, Sirrs S, Marfa MP, Vanier MT, Walterfang M, Bolton S, Dawson C, Héron B, Stampfer M, Imrie J, Hendriksz C, Gissen P, Crushell E, Coll MJ, Nadjar Y, Klünemann H, Mengel E, Hrebicek M, Jones SA, Ory D, Bembi B, Patterson M; International Niemann-Pick Disease Registry (INPDR). Consensus clinical management guidelines for Niemann-Pick disease type C. Orphanet J Rare Dis. 2018 Apr 6;13(1):50. doi: 10.1186/s13023-018-0785-7. PMID: 29625568; PMCID: PMC5889539.

71. Villani M, Subathra M, Im YB, Choi Y, Signorelli P, Del Poeta M, Luberto C. Sphingomyelin synthases regulate production of diacylglycerol at the Golgi. Biochem J. 2008 Aug 15;414(1):31-41. doi: 10.1042/BJ20071240. PMID: 18370930; PMCID: PMC5125090.

72. Kamiya Y, Mizuno S, Komenoi S, Sakai H, Sakane F. Activation of conventional and novel protein kinase C isozymes by different diacylglycerol molecular species.

Biochem Biophys Rep. 2016 Jul 20;7:361-366. doi: 10.1016/j.bbrep.2016.07.017. PMID: 28955926; PMCID: PMC5613651.

APPENDIX A: CELL LINES USED

Cell line:	Description:	Karyotype:
A549	Adenocarcinoma human alveolar basal epithelial cells	Hypotriploid
HBEC3-KT	Human epithelial lung bronchial cells	Diploid/tetraploid